**Atmospheric
Chemistry
and Physics**

Impacts of climate change on air pollution levels in the Northern Hemisphere with special focus on Europe and the Arctic

G. B. Hedegaard[1,2], J. Brandt[1], J. H. Christensen[1], L. M. Frohn[1], C. Geels[1], K. M. Hansen[1], and M. Stendel[2]

[1]National Environmental Research Institute, University of Aarhus, Roskilde, Denmark
[2]Danish Climate Center, Danish Meteorological Institute, Copenhagen, Denmark

Abstract. The response of a selected number of chemical species is inspected with respect to climate change. The coupled Atmosphere-Ocean General Circulation Model ECHAM4-OPYC3 is providing meteorological fields for the Chemical long-range Transport Model DEHM. Three selected decades (1990s, 2040s and 2090s) are inspected. The 1990s are used as a reference and validation period. In this decade an evaluation of the output from the DEHM model with ECHAM4-OPYC3 meteorology input data is carried out. The model results are tested against similar model simulations with MM5 meteorology and against observations from the EMEP monitoring sites in Europe.

The test results from the validation period show that the overall statistics (e.g. mean values and standard deviations) are similar for the two simulations. However, as one would expect the model setup with climate input data fails to predict correctly the timing of the variability in the observations. The overall performance of the ECHAM4-OPYC3 setup as meteorological input to the DEHM model is shown to be acceptable according to the applied ranking method. It is concluded that running a chemical long-range transport model on data from a "free run" climate model is scientifically sound. From the model runs of the three decades, it is found that the overall trend detected in the evolution of the chemical species, is the same between the 1990 decade and the 2040 decade and between the 2040 decade and the 2090 decade, respectively.

The dominating impacts from climate change on a large number of the chemical species are related to the predicted temperature increase. Throughout the 21th century the ECHAM4-OPYC3 projects a global mean temperature increase of 3 K with local maxima up to 11 K in the Arctic winter based on the IPCC A2 emission scenario. As a consequence of this temperature increase, the temperature dependent biogenic emission of isoprene is predicted to increase significantly over land by the DEHM model. This leads to an increase in the O_3 production and together with an increase in water vapor to an increase in the number of free OH radicals. Furthermore this increase in the number of OH radicals contributes to a significant change in the typical life time of many species, since OH are participating in a large number of chemical reactions. It is e.g. found that more SO_4^{2-} will be present in the future over the already polluted areas and this increase can be explained by an enhanced conversion of SO_2 to SO_4^{2-}.

1 Introduction

Recently, there has been a growing interest in the effects of climate change on the future air pollution levels. It is well known that the composition of the atmosphere will change due to climate related changes in anthropogenic emissions. According to the newly released IPCC report (Solomon et al., 2007) some meteorological parameters will also change in the future due to the man-made changes of the composition of the atmosphere. A general temperature increase will affect many if not all other meteorological parameters. Since the distribution of air pollution is highly dependent on meteorology it is hypothesized that the air pollution levels and spatial distribution even with unchanged anthropogenic emissions will be changed in a warmer climate. To estimate the changes in the air pollution levels in the future solely due to climate change requires complex computer models.

Until now, a great number of sensitivity studies of the effect from specific meteorological parameters on air pollution distribution has been carried out, see e.g. Zlatev and Brandt (2005). In these studies for example the temperature alone has been altered to suit different temperature scenarios. Sensitivity studies makes it possible to get a rough overview of the effect of a specific meteorological parameter on the air pollution. However, to include all effects of a changing

Correspondence to: G. B. Hedegaard
(gbh@dmu.dk)

climate much more complicated modelling tools are needed. Using predicted temperature increases for year 2100, a recent study by Guenther et al. (2006) indicates that the isoprene emissions could increase by a factor of two. Such estimates are, however, very uncertain and other studies have shown (e.g. Monson et al., 2007) that more sophisticated approaches including the impact of e.g. increasing CO_2 concentrations and changes in precipitation are needed in order to predict future emissions of biogenic VOCs.

The hemispheric Chemical long-range Transport Model (CTM) DEHM (Danish Eulerian Hemispheric Model) (Christensen, 1997; Frohn et al., 2002b, 2003; Frohn, 2004) is used in the current experiment to investigate the future air pollution levels and distribution in the Northern Hemisphere with special emphasis on Europe and the Arctic. The coupled Atmosphere-Ocean General Circulation Model ECHAM4-OPYC3 (Roeckner et al., 1999; Stendel et al., 2002) provides 21st century meteorology and part of the 20th century based on the IPCC SRES A2 scenario (Nakicenovic et al., 2000) every 6 h as input to DEHM. In order to save computing time the experiment is focused on three decades instead of simulating the 21st century in one continuous run. The three periods are; 1990–1999, 2040–2049 and 2090–2099. These three time-slices are simulated with constant 1990 anthropogenic emissions in order to separate out the effects on air pollution from climate change. The biogenic emissions of isoprene is allowed to vary in the experiments. The meteorology in these three simulations are all based on ECHAM4-OPYC3 and the time periods are the 1990s, the 2040s and the 2090s, which are assumed to represent the changes in the 21st century.

Nearly all processes involved in the chemical composition of the atmosphere depend on temperature, humidity and cloud cover and therefore will be affected by climate change. Atmospheric transport and transport patterns including the horizontal and vertical mixing is directly determined by the different weather parameters as e.g. wind, convection, mixing properties in the Atmospheric Boundary Layer (ABL), solar radiation, temperature, heat fluxes, etc. The atmospheric chemical reactions and photolysis rates are dependent on e.g. the humidity, global radiation as function of the cloud cover and type, temperature, albedo, etc. Furthermore, the precipitation frequency and amount as well as the surface properties have great influence on the wet and dry deposition levels. Finally there are several parameters that have a large influence on the emissions, e.g. the temperature dependence of natural emissions of volatile organic compounds (VOC) and the temperature dependence of anthropogenic emissions through domestic heating, power consumption, agriculture etc. Natural emissions of NO_x also depend on the weather parameters like e.g. lightning or soil temperatures. Therefore it is hypothesized that a changed future climate will have an impact on future levels and distribution of air pollution concentrations and deposition of chemical species in the Northern Hemisphere. To test this hypothesis several questions have to be answered first.

There are two main steps in this experiment. First of all it is assumed that the Atmosphere-Ocean General Circulation Model ECHAM4-OPYC3 is able to provide a realistic and consistent picture of the meteorological key parameters applied in the air pollution model. On the basis of this assumption the first step is to justify that it makes sense to drive an air pollution model with data from a "free run" climate model. Hereafter the meteorological parameters that are changing due to climate change are identified, and from knowledge of the air pollution chemistry and climate change, the effects on the air pollution distribution and levels in the future are estimated. The second step in this experiment is to analyse the output data from the air pollution model. Since DEHM includes a chemical scheme with 63 chemical species, there is a great amount of data to analyse from the output of the simulations carried out here. Therefore only some selected chemical species are analysed with respect to the key meteorological parameters.

The number of specific hypotheses that can be tested and questions that can be answered using the one-way coupled climate-chemical transport model system setup is large. Many of these specific hypotheses can only be answered by running the DEHM model a large number of times to do scenario- or sensitivity studies. The main objectives of the experiment carried out here is therefore limited to test the method of doing a one-way coupling of a climate model and a chemical transport model and to identify and investigate some of the most important processes involved in the impacts from global change on air pollution levels and distribution in the 21st century.

A description of the models used in this work and a description of the EMEP monitoring network which the results in this analysis is evaluated against is included in Sect. 2. In Sect. 3 the method of the model coupling is documented. Section 5 includes the validation of the method and the scenario results and discussion of the sensitivity of the selected species is provided in Sect. 6. The conclusions and suggestions to future work are summarized in Sect. 7.

2 Model descriptions

In this section the numerical, physical and chemical characteristics of the chemical long-range transport model DEHM and the climate model ECHAM4-OPYC3, will be summarized.

2.1 The atmosphere-ocean general circulation model, ECHAM4-OPYC3

As the name ECHAM4-OPYC3 indicates, this general circulation model consists of an atmosphere (ECHAM4) and an ocean component (OPYC3).

The atmosphere component (ECHAM4) is horizontally defined in a spectral grid with truncation T42 (T42

corresponding roughly to a $2.8° \times 2.8°$ transformed grid). Vertically the model is defined in a hybrid sigma-pressure system and divided into 19 layers extending from the surface of the earth to the 10 hPa pressure level. The concentrations of greenhouse gases and halocarbons as well as the surface sulphur emissions are prescribed in the model according to the IPCC SRES A2 scenario, which assumes a regionally limited cooperation and slower adaption of new technologies, together with an unstabilized population growth (Nakicenovic et al., 2000). The tropospheric sulphur concentrations are calculated interactively within the atmosphere model by including a simplified sulphur model. This sulphur model is driven by the surface emissions from the SRES A2 scenario and by internally calculated processes such as sulphur chemistry, transport and deposition (for further details see Roeckner et al., 1999). With respect to the experiment carried out here, the inclusion of a sulphur model in the ECHAM4-OPYC3 model only acts to improve the description of global radiation and therefore the weather parameters used as input to the chemical transport model DEHM. The SO_2 and SO_4^{2-} levels studied in the final results from this experiment are solely generated in the chemical long-range transport model, and are therefore only indirectly (through meteorology) affected by the SO_2 concentration model in the ECHAM4-OPYC3. The transport of water vapor, cloud water and chemical constituents is calculated with a semi-Lagrangian scheme following Williamson and Rasch (1994). For further details about the physics of the model see Roeckner et al. (1996).

The ocean component of the Atmosphere-Ocean General Circulation Model is an extended version (level 3) of the OPYC model (Oberhuber, 1993). The ocean model consists of three submodels: an interior ocean, a surface mixed layer and a sea ice component. Vertically the model is divided into 11 layers and poleward of $36°$ the horizontal resolution is truncated at T42, which is identical to the atmosphere model. For lower latitudes (equatorward of $36°$ latitude) the meridional resolution is gradually decreased to $0.5°$ at the equator (Roeckner et al., 1999). For details about the dynamics of the three submodels see Roeckner et al. (1999).

The coupling of the three oceanic submodels are carried out quasi-synchronously and they exchange information once a day. The atmosphere model provides daily-averaged surface fluxes of momentum, heat and fresh water to the ocean model, which returns daily-averages of the sea surface temperatures, ice momentum and concentration as well as the ice and snow thickness.

2.1.1 Forcings

The meteorological output data is the result from a 240-year long ECHAM4-OPYC3 simulation with time-dependent forcing. The simulation is only forced with respect to the concentrations of greenhouse gases, halocarbons and SO_2. In the period 1860–1990, the concentrations are derived from observations and for the period 1990-2100, they are prescribed according to the IPCC SRES A2 scenario. The emissions following the A2 scenario are given every ten years and are linearly interpolated in time. Furthermore, the tropospheric O_3 distribution is allowed to vary as a result of prescribed concentrations of anthropogenic precursor gases CH_4, NO_x, CO and to stratospheric O_3 and NO_x whose concentrations are given for 1860, 1985 and 2050. Intermediate values are then calculated by linear interpolation, and from 2050 onwards the concentration is held constant at the 2050 level (Roelofs and Lelieveld, 1995).

2.2 The predicted meteorology of the 21st century

The total forcing from all greenhouse gases results in an increase in radiation from $2.0 \, W/m^2$ to $8.1 \, W/m^2$ with respect to pre-industrial values according to the A2 emission scenario which these simulations are based on. Sulphur emissions are projected to increase by 50% until the 2030s, after which they gradually decrease to present day level in year 2100 (Nakicenovic et al., 2000).

The global average temperature is found to increase by 3 K during the 21st century, which is in good agreement with previous studies (Stendel et al., 2002). There are large seasonal and regional differences in this warming with values up to 11 K during winter in the Canadian and Siberian Arctic. For annual means, the largest increase is projected over Greenland and the sub polar regions of Asia, North America and Europe. In these areas the annual temperature increase exceeds 6 K (Stendel et al., 2002). In good agreement with other studies the diurnal temperature range decreases and the warming over land is significantly larger compared to the warming over the ocean (Stendel et al., 2002). The sea ice in the Arctic is estimated to retreat by approximately 40%. Particularly, over the Barents Sea, the sea ice is predicted to vanish completely by the end of the century.

The globally averaged precipitation only changes slightly. However, there are huge regional and seasonal differences. Winter precipitation over the temperate and Arctic regions increases by 10–50%, whereas the precipitation generally decreases over the subtropics and mid-latitudes, which is in good agreement with other studies. Finally concerning the mean sea level pressure this ECHAM4-OPYC3 simulation results in a shift towards a higher North Atlantic Oscillation index (Stendel et al., 2002). Both the Icelandic low and the Azores high are slightly enhanced making the differences larger and thereby the NAO index more positive.

2.3 The chemical transport model, DEHM

The chemical long-range transport model DEHM (Danish Eulerian Hemispheric Model) has been under development since the beginning of the 1990's at the National Environmental Research Institute (NERI), see (Christensen, 1997; Frohn et al., 2002b, 2003; Frohn, 2004). For general
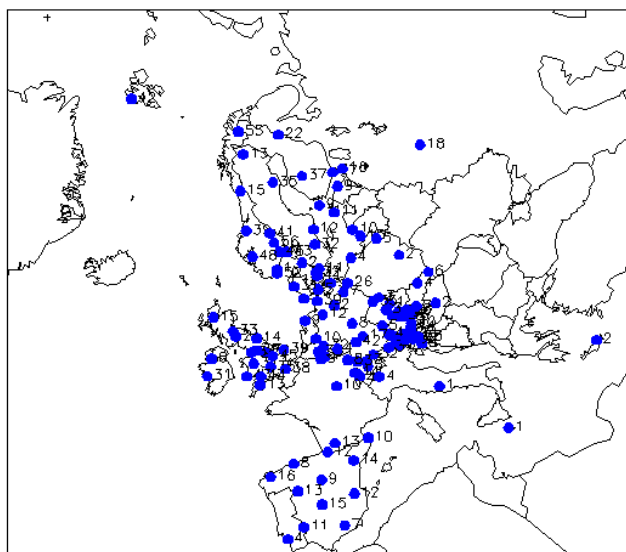
Fig. 1. The EMEP measurement network 2001 (www.emep.int).

documentation and validation of the model performance see Christensen (1997), Frohn (2004), Geels et al. (2004), van Loon et al. (2004), Brandt et al. (2005) and van Loon et al. (2007).

The DEHM model is a terrain-following model based on a set of coupled 3-D-advection-diffusion equations. Horizontally the domain covers the majority of the Northern Hemisphere with a resolution of $150 \, \text{km} \times 150 \, \text{km}$ (the domain can be seen in Figs. 4–14).

The temporal resolution in the model (the time step) is variable and dependent on the Courant-Friedrich-Lewi stability criteria. Under normal conditions the time step varies between 1200 s and 1400 s. The model results are saved every 1 h and thereafter re-sampled to the needed average values used in the statistical evaluation.

The DEHM is defined in sigma coordinate system and is divided into 20 irregular distributed layers extending from the earths surface to the 100 hPa pressure level. The resolution is highest close to the surface, and ranging from approximately 50 m between the layers in the boundary layer, to approximately 2000 m between the layers at the top of the domain (see Table 4.1 p. 28 in Frohn (2004)). This distribution of layers gives the model approximately 7 layers in the boundary layer, 10 layers in the free troposphere and finally approximately 3 layers in stratosphere. For further details about the physical parameterizations and the numerical methods of the model see, Christensen (1995), Christensen (1997), Frohn (2004) and Hedegaard (2007).

The chemical scheme of the DEHM model is an explicit scheme and it is based on the scheme of the EMEP model (Frohn, 2004; Brandt et al., 2005). The DEHM chemical scheme includes the chemistry of 63 different chemi-

cal compounds. These 63 chemical species participates in a large number of chemical processes and 120 of these are included in the present version of the CTM model (Frohn, 2004; Brandt et al., 2005). The model includes e.g. SO_x, NO_x, O_3, CO, NH_x, many VOCs and primary and secondary inorganic particles, $PM_{2.5}$, PM_{10}, Total suspended Particles (TSP), Sea Salt, SO_4^{2-}, NO_3^-, NH_4^+). For a full list of all the chemical species and the included chemical reactions see Frohn (2004).

The performance of the present and earlier versions of DEHM model has been widely tested (Christensen, 1993, 1995, 1997; Brandt et al., 2001a,b; Frohn et al., 2002a,b, 2003; Frohn, 2004; Geels et al., 2004). The DEHM model has participated in several model inter-comparison projects see e.g. van Loon et al. (2007).

The anthropogenic emissions used in the present version of the DEHM model consist of a combined set of data (see Frohn (2004) for details). The emissions of the primary pollutants consist of data from the Global Emission Inventory Activity (GEIA) (Graedel et al., 1993), the Emission Database for Global Atmospheric Research (EDGAR) (Olivier et al., 1996) both with $1° \times 1°$ spatial resolution and finally data from the European Monitoring Evaluation Programme (EMEP) (Vestreng, 2001) for Europe with a $50 \, \text{km} \times 50 \, \text{km}$ resolution. All emission data are provided as annual values. The emission data is divided into 12 different emission types which vertically is released in different specified levels of the model similar to the emission release in the EMEP-model. Temporally the annual emissions are re-distributed into seasonal and diurnal variations similar to the EMEP model. For further details see Simpson et al. (2003). In DEHM, the GEIA natural VOC emission model is included to account for the biogenic emissions of isoprene (Guenther et al., 1995).

2.4 EMEP measuring network

In order to validate the DEHM model performance with ECHAM4-OPYC3 meteorology, comparisons has been made with earlier simulations using MM5 meteorology (Grell et al., 1995) and observations of concentrations of chemical compounds. The observations used for this validation originates from the EMEP measuring network, which includes a large number of chemical components (Hjellbrekke, 2000). The location of the specific measuring sites are shown in Fig. 1. Not all measuring sites are measuring all the validated chemical components all the time. For details about the measurement period and frequency of the individual components see Hjellbrekke (2000).

3   Experimental design

The model setup is straight forward. The ECHAM4-OPYC3 provides a number of meteorological parameters

(e.g. geopotential height, temperature, wind components, surface pressure etc.) which are used as meteorological input to the DEHM model. However, several pre-processing have to be carried out before the data from ECHAM4-OPYC3 climate model can be implemented as meteorological data in the DEHM model.

In the present version of the DEHM model, the mixing height is derived from the turbulent kinetic energy TKE. However, this parameter was not saved in the climate simulations applied here. Therefore the mixing height is based on a simple energy balance equation for the internal boundary layer (cf. Christensen, 1997). The mixing height parameterization has been used before in earlier versions of the DEHM model and it is documented to perform quite well (Brandt, 1998).

The ECHAM4-OPYC3 provides data every six hours to the DEHM model. The differences in both temporal and spatial resolution between the two models results in the necessity of a transformation of data in time and space.

A year in the ECHAM4-OPYC3 model is only 360 days long. In order to compare the data from the ECHAM4-OPYC3-DEHM simulations with MM5-DEHM simulation and with observations in the validation, interpolations has been made according to the method used in the PRUDENCE project (Christensen, 2005).

The numerical weather prediction model MM5 is normally used as a meteorological driver for the DEHM model. The MM5 model provides short term forecast of the real weather based on global data from the ECMWF as usually done in weather forecasting systems. In this case the MM5 model is used to calculate gridded data for DEHM as six hour forecasts and therefore used as an intelligent interpolator between the global data which is provided every six hours. In this way the DEHM results based on the MM5 meteorological data gives a realistic simulation of the air quality conditions.

The evaluation of the climate driven air quality simulations is carried out as a comparison with the realistic simulation based on MM5. In the paper we show that we are able to reproduce annual/decadal mean values and seasonal variations using the climate driven air quality simulation compared to the realistic simulation and compared to measurements. This is a significant result, which proves that the climate driven air quality simulations does not give systematic errors.

To test the validity of the one-way coupling method and to produce results, five ten-year long simulations have been carried out. The first two of these simulations are used to test the scientific foundation of this experiments: One simulation is based on MM5 (Grell et al., 1995) meteorology and one simulation is based on ECHAM4-OPYC3 (Stendel et al., 2002) meteorology. Both simulations are carried out for the period 1990–1999 and are forced with the real emissions of this period. The basic idea behind these two simulations is to test the model results against measurements of air pollution in the 1990s. After this evaluation three simulation of the three time-slices of the future century is carried out.

4 Statistical methodology

The comparison of data has been performed by inspection of measures for the averages and the variability of the data. The statistical parameters calculated here are the mean ($\overline{P}$) and the fractional bias (FB), which represents the average values, the correlation coefficient ($\hat{r}$), which represents the variability in the data series and finally the normalized mean square error (NMSE), which represent both the averages and variability of the data.

4.1 Statistical formulas

If P is the predicted value, the mean is defined by

$$\overline{P} = \frac{1}{N} \sum_{i=1}^{N} P_i \tag{1}$$

where N is the total number of predicted values in each data series Taylor (1997).

The fractional bias is defined as

$$\text{FB} = 2 \frac{\overline{P} - \overline{O}}{\overline{P} + \overline{O}} \tag{2}$$

In Eq. (2) P refers to the predicted value (of the DEHM ECHAM4-OPYC3 simulation and the DEHM MM5 simulation) and O refers to the observed value.

As mentioned above, the correlation coefficient ($\hat{r}$) and the normalized mean square error (NMSE) are calculated to give an estimate of how well the model simulates the variability of the data compared to measurements.

The correlation coefficient is given as the covariance between the two series of deviation from their respective means, divided by their respective standard deviations

$$\hat{r} = \frac{\sum_{i=1}^{N} (O_i - \overline{O})(P_i - \overline{P})}{\sqrt{\sum_{i=1}^{N} (O_i - \overline{O})^2 \sum_{i=1}^{N} (P_i - \overline{P})^2}} \tag{3}$$

The normalized mean square error gives a measure of the overall deviation between the observed and the predicted values

$$\text{NMSE} = \frac{1}{N \cdot \overline{O} \cdot \overline{P}} \sum_{i=1}^{N} (P_i - O_i)^2 \tag{4}$$

4.2 Two-tailed t-test

In order to conclude whether two model simulations are significantly different from one another the t-test for change in mean values has been performed Spiegel (1992). If $\overline{P_1}$ denotes the mean of one data series and $\overline{P_2}$ denotes the mean of another data series the hypothesis H_0 has to be tested

$$H_0 : \overline{P_1} = \overline{P_2} \tag{5}$$

If the hypothesis can be rejected, one can conclude that the mean values of the two time series are not equal, which in this case means that there is a change in the mean values. To test the hypothesis H_0 the t-statistic (t) is calculated the following way;

$$t = \frac{\overline{P_1} - \overline{P_2}}{\sigma\sqrt{\frac{1}{N_1} + \frac{1}{N_2}}} \text{ where } \sigma = \sqrt{\frac{N_1 s_1^2 + N_2 s_2^2}{N_1 + N_2 - 2}} \qquad (6)$$

Here N_1 and N_2 denotes the number of degrees of freedom of the two data sets and s_1 and s_2 denotes the standard deviations given by Spiegel (1992)

$$s = \sqrt{\frac{1}{N}\sum_{i=1}^{N}(x_i - \overline{x})^2} \text{ where } \overline{x} = \frac{1}{N}\sum_{i=1}^{N} x_i \qquad (7)$$

Whether the hypothesis can be rejected or not, can now be looked up in a t-distribution table, see e.g. Malmberg (1985). The number of degrees of freedom is defined as (N_1+N_2-2) because it is the number of independent observations (the length of the time series) minus the number of statistical parameters, which is being estimated from these observations. That means, when comparing the results of the ECHAM4-OPYC3 simulation with the results of the MM5 simulation for the control period 1990–1999, there are 10 years or so-called observations in each simulation and two statistical parameters (e.g. the mean value of each of the two observation sets), which lead to the definition; # degrees of freedom $=(N_1+N_2-2)=10+10-2=18$, which is used above.

As the header of this subsection indicates, the t-test here is two-tailed. This simply means, that when the hypothesis H_0 is rejected, two alternative hypothesis's can be accepted. In the case of the test of mean value, the following two acceptance hypothesis's are a) the difference in mean value of the two data set are significantly positive or b) the difference in mean value of the two data set is significantly negative. The fact that there are two alternative hypothesis's to accept, makes the t-test two-tailed.

4.3 The ranking method

Ranking is a good evaluation method of model performances, when different model simulations have been carried out. The method was e.g. used in the ETEX ATMES-II model exercise performance comparison (see e.g. Mosca et al., 1997). In the validation process it is most convenient to compare the two simulations of the control period (1990–1999) with variable emissions, because these results then can be compared to real measurements. This comparison enables the evaluation of the ECHAM4-OPYC3 DEHM setup vs real observations and relative to another model setup (MM5 DEHM) which already is documented to perform well (Christensen, 1993, 1995, 1997; Frohn et al., 2002a,b, 2003; Frohn, 2004; Brandt et al., 2001b; Geels et al., 2004).

First the correlation coefficient, the fractional bias and the normalized mean square error have been calculated for the precipitation, as well as the wet depositions and concentrations of several chemical species.

In consistency with the ranking method used by Brandt et al. (1998), a local ranking has been performed for each model characteristics and for each statistical parameter. This means, that the best performing parameter of two simulations has been given the value 1 and the second best the value 2. In the case of two equal performing parameters, both have been given the value 1. Each statistical parameter of each characteristics has been given the same weight in this analysis.

After the local ranking of each statistical index, a global ranking has been calculated as the sum of the local rank. In this way, the result with the smallest global rank indicates the best performing model in terms of model results compared to measurements.

5 Validation of the experimental method for the period 1990–1999

In Figs. 2 and 3 examples of the comparison between measured and predicted chemical species applied in the validation are shown. The EMEP measuring network provides diurnal mean or accumulated observational data of the following chemical species: NH_3, NH_4^+, sum of NH ($=NH_3+NH_4^+$), HNO_3, NO_3^-, sum of NO ($=HNO_3+NO_3^-$), NO_2, O_3, SO_2, SO_4^{2-} and finally the diurnal max. and hourly O_3. Furthermore the precipitation as well as the wet deposition of NH_4^+, NO_3^- and SO_4^{2-} are available. Since the model performance is different from one chemical species to another, the analysis is carried out species by species. This is due to the fact that some species are subject to long-range transport while others are short-lived and some deposit locally.

The validation analysis is based on monthly mean values of simulated and measured data. The data have therefore been re-sampled from the daily values, since it does not make sense to validate climate model results on a day to day basis. It is expected that the climate model is able to simulate the seasonal variations, and therefore the analysis is based on monthly mean values. Furthermore the data have been averaged over space meaning that for every day a mean value has been made over all the measurement sites (both for measurements as well as for model results). The daily time series has afterwards been averaged to monthly mean values.

An analysis of the concentration of nitrogen dioxide (NO_2) is shown in the first panel of Figs. 2 and 3. For both the MM5 and the ECHAM4-OPYC3 setup, the predicted data underestimates the observed value. This is probably due to the relative low resolution of the DEHM model. There are large differences in measured NO_2 concentrations between urban and rural areas. The concentration of NO_2 is much higher in urban areas, where it primary is emitted. With a resolution of $150\,km\times150\,km$, the DEHM model is not expected
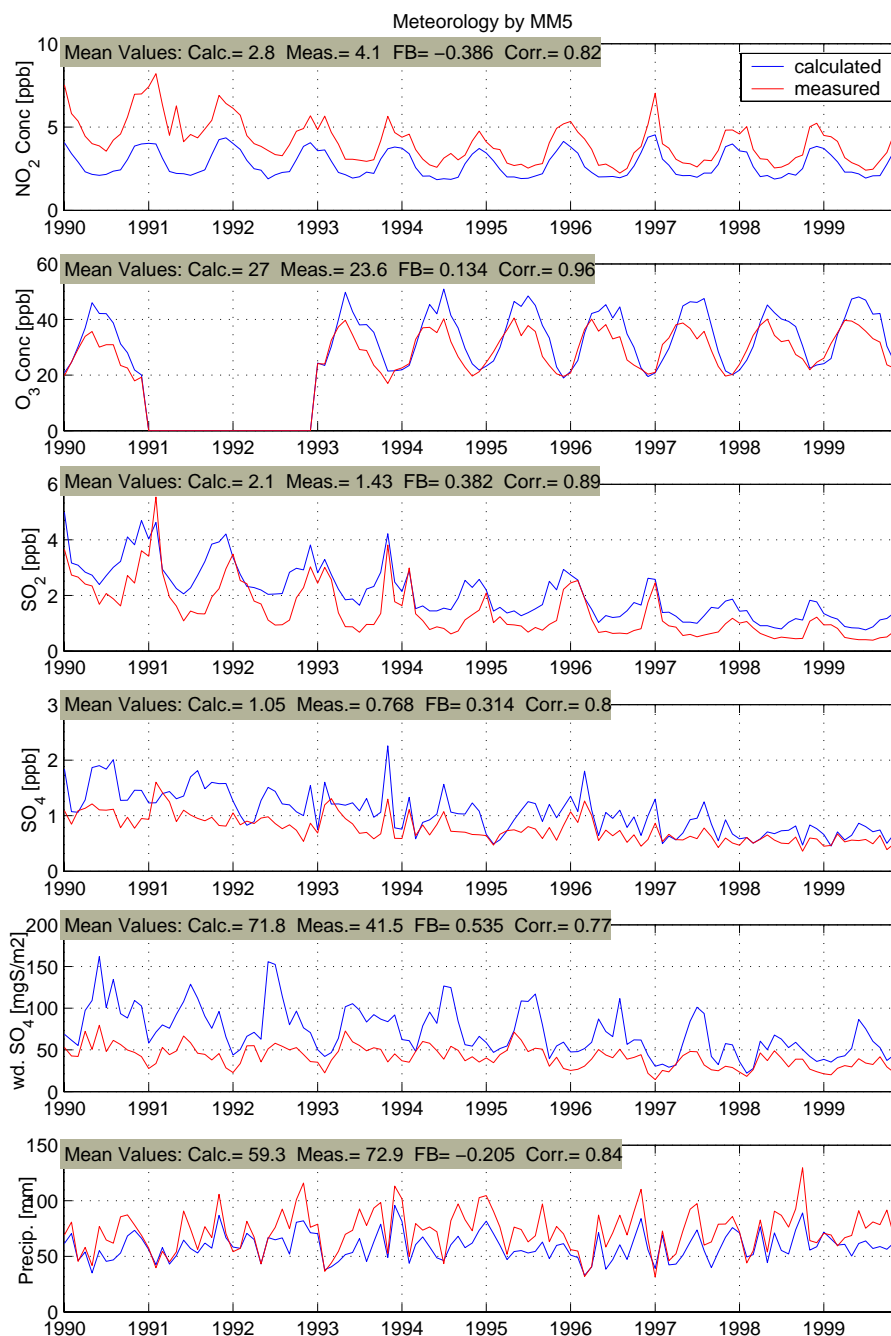
Fig. 2. The calculated concentrations of NO_2, O_3, SO_2 and SO_4^{2-} as well as wet deposition of SO_4^{2-} and precipitation is compared with the observations from the EMEP measurement network (cf. Sect. 2.4) for the period 1990–1999. The data are monthly averaged values averaged over all the available measurement sites. The simulation is based on MM5 meteorology plus and 1990–1999 emissions. Also the mean values of the calculated and measured time series, the fractional bias (FB) and the correlation coefficient (Corr.) between the measured and calculated data series are displayed in each panel. For O_3 measurements are not available in 1991 and 1992.

to resolve the urban areas very well. The model prediction will simply smooth the high urban emissions over a large area and therefore the resulting model prediction is underestimating the concentration of nitrogen dioxide. The results

of Frohn (2004) support this finding. In Frohn (2004) an earlier version of the DEHM model, it is used in a nested mode with two different nests. From these simulations it is found that the underestimation of the NO_2 in the model decreases
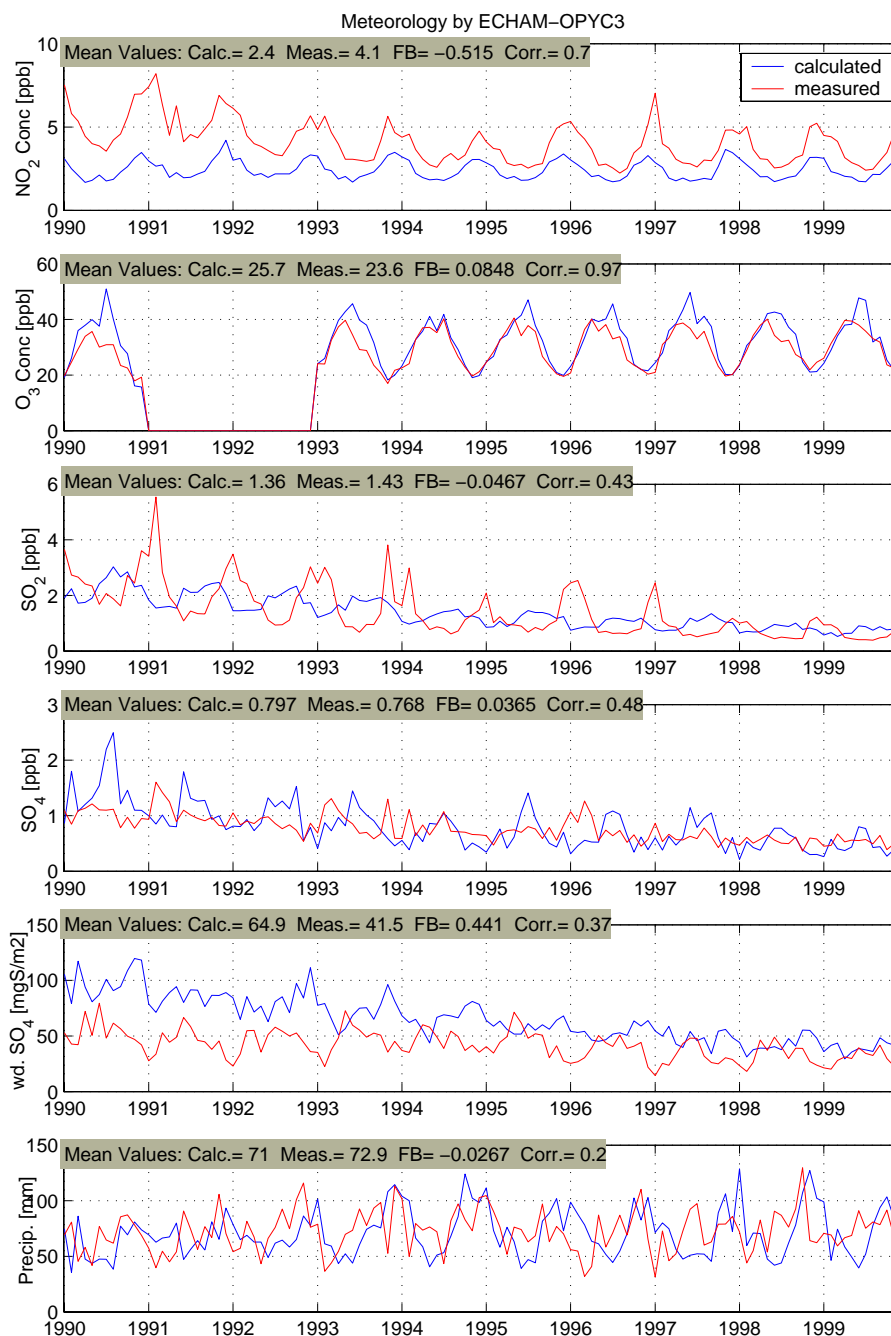
Fig. 3. As in Fig. 2, but with the simulations based on ECHAM4-OPYC3 meteorology.

with increasing resolution. The correlation coefficient is high with respect to the prediction of the concentration of nitrogen dioxide for both model setups. However, it is highest in the case of the MM5 setup.

In the second panel of Figs. 2 and 3, the concentration of ozone (O_3) is shown. Here it should be mentioned that the missing data in 1991 and 1992 is due to an error in the obser-

vation set used for this analysis. However, the missing data is not expected to change the results of this analysis. In the case of the ECHAM4-OPYC3 model setup, the prediction of mean and variability in the ozone concentration is very good. Also the correlation is very high in the MM5 setup, however here the fractional bias is somewhat larger than in the case of ECHAM4-OPYC3 setup. There is a tendency of the DEHM

model to overestimate the high concentration episodes during the spring. This feature is present in both model setups and therefore likely to be independent of the meteorological input. The measurements of the O_3 concentration are collected at the surface level. In contrast the predicted O_3 concentration represent an average value of the air column in between the lowest layers of the model. This means an average value of the lowest approximately 50 m of the atmosphere. The real profile of O_3 is very steep in the lowest 50 m of the atmosphere, especially during high concentration events. This explains the tendency of the model to underestimate the high peak events in summertime. A solution to this problem could be to prescribe an O_3 profile in the lowest layers of the model. However, this is presently not included in the DEHM model.

The concentration of sulphur dioxide (SO_2) is shown in the third panel of Figs. 2 and 3. The ECHAM4-OPYC3 model setup succeeds to predict the mean level very well, whereas the results of the MM5 based simulation show a tendency to over-predict the mean concentration of SO_2. Only the MM5 model setup predicts the correlation successfully. In both figures the decreasing emission of SO_2 during the 1990s can be observed.

Sulphate is displayed in the fourth panel of Figs. 2 and 3. The results here are very similar to what was found for SO_2. The results of the MM5 based simulation tend to overestimate the mean level. However, the data correlates very well with the observations. In contrast the ECHAM4-OPYC3 setup has the mean level right. However, the predicted data do not correlate with the observations. During the 1990s the anthropogenic emission of SO_2 has been reduced significantly and this reduction is visible in the SO_4^{2-} concentration because of the close relation between these two chemical species.

The two lowest panels of Figs. 2 and 3 display the wet deposition of (SO_4^{2-}) and the precipitation. Here both model setups overpredict the mean level of wet deposition of SO_4^{2-}. The MM5 model setup correlates acceptably well with the measurements in contrast to the climatic weather simulation (ECHAM4-OPYC3) which only show very low correlation with observed data. It could be expected that the tendency of both the model setups to overpredict the wet deposition of SO_4^{2-} originates in the prediction of the precipitation, since the same tendency is not generally present in the concentration plots of sulphate. However, inspecting the precipitation plots (the lowest panel of these figures), reveals that precipitation level is not overpredicted in the two simulations. It is rather the opposite. The precipitation plot shows only the amount of precipitation. However, the timing relative to concentration levels, the frequency of precipitation events and finally the type of precipitation, also have large influence on the level of wet depositions.

Considering the precipitation plot alone, the ECHAM4-OPYC3 simulation definitely fails to describe the measured

variation in precipitation, but it does have a seasonal variation and the mean levels fit very well. The failure in correlation is not surprising since the ECHAM4-OPYC3 weather is solely climatic and therefore it cannot be expected to simulate the timing of the real weather. Analysing the results based on MM5 meteorology, the mean level is actually worse represented by the MM5 model than by ECHAM4-OPYC3. On the other hand the correlation of the results of the MM5 model setup compared to measurements is high, which was expected since MM5 is a day-to-day weather forecast model in contrast to ECHAM4-OPYC3.

The precipitation level of the ECHAM4-OPYC3 model setup is very similar to the precipitation measurements of the EMEP stations both in the summer and the winter. This indicates that it is precipitation timing and/or frequency and/or type, which differs from the observations with respect to the discussion about wet deposition above. When performing an analysis including a comparison of results at a limited number of measurement stations, there is also a risk that these stations do not represent the average observed weather and chemistry over Europe. Furthermore, the individual measurements only represent a point, whereas the predicted values from the two simulations represent areas (grid cells). This will inherently introduce some uncertainties in the analysis carried out here.

5.1 Ranking

The purpose of this analysis is to document the performance of the model setup ECHAM4-OPYC3 DEHM. In this connection the ranking method (see Sect. 4.3) is used to validate the performance of the climate ECHAM4-OPYC3 DEHM setup vs. the usual forecast MM5 DEHM setup.

In Table 1 the ranking results of the MM5 setup versus the ECHAM4-OPYC3 setup for the year 1990 is shown. The ranking has been performed for the correlation coefficient (Corr.), the fractional bias (FB) and the normalized mean square error (NMSE) of each of the chemical species (from the EMEP network). Each statistical index has been given the value one for best performance and the value two for second best performance and all these local ranks are added up to a total rank for each statistical parameter of each simulation. The "global rank" is calculated as the sum of all total ranks for each simulation. If the global ranks of the two model simulations are similar, it can be concluded that the two simulations have received a similar number of one's and two's and therefore have similar performance with respect to the individual statistical parameters. In general, a lower global rank means a better performance. The MM5 model setup "wins" with 61 points. However, it is marginal which determines the outcome since the ECHAM4-OPYC3 setup is nearly just as good with a global rank for year 1990 of 65.

The rest of the years in the 1990 decade show similar results to the result presented in Table 1. However, it is alternating which of the model setups has the best ranking (for

Table 1. Example of validation of one year of the data from the DEHM simulation based on MM5 meteorology and the DEHM simulation based on ECHAM4-OPYC3 meteorology. The correlation coefficient (Corr.), the fractional bias (FB) and normalized mean square error (NMSE) of the monthly mean values of year 1990 and ranking of these statistical parameters are calculated and shown. With respect to ozone, both the diurnal average (MEAN), the hourly average (HOUR) and the diurnal maximum (DM) concentration of ozone are included in the table.

	Corr.				Fb				NMSE			
Chemistry	MM5	Rank	ECHAM	Rank	MM5	Rank	ECHAM	Rank	MM5	Rank	ECHAM	Rank
NH_4^+	0.72	1	0.70	2	0.19	2	0.10	1	0.28	2	0.27	1
SUM NH	0.78	2	0.80	1	−0.35	1	−0.48	2	0.55	1	0.69	2
WD. NH_4^+	0.51	1	0.49	2	0.20	1	−0.23	2	0.54	1	0.63	2
PREC	0.71	1	0.48	2	−0.16	2	−0.20	1	0.26	1	0.32	1
NO_3^-	0.57	2	0.69	1	0.12	2	−0.11	1	0.34	2	0.33	1
SUM NO	0.85	2	0.91	1	0.10	2	0.01	1	0.22	2	0.14	1
WD. NO_3^-	0.67	1	0.51	2	0.58	2	0.01	1	0.64	2	0.38	1
NO_2	0.45	2	0.49	1	−0.61	1	−0.79	2	1.30	1	1.80	2
SO_2	0.52	1	0.5	2	0.29	2	−0.09	1	0.86	2	0.72	1
SO_4^{2-}	0.63	1	0.54	2	0.40	2	0.35	1	0.57	2	0.52	1
WD. SO_4^{2-}	0.54	1	0.37	2	0.64	1	0.65	2	0.93	1	1.20	2
O_3 MEAN	0.23	1	0.08	2	0.19	2	0.19	1	0.08	1	0.10	2
O_3 HOUR	0.2	1	0.02	2	0.20	2	0.17	1	0.09	1	0.10	2
O_3 DM	0.51	1	0.45	2	0.01	1	0.02	2	0.02	1	0.03	2
Total Rank		18		24		23		19		20		22
Global Rank	MM5	ECHAM										
	61	65										

further details see Hedegaard, 2007). Summing up all the results from all the years, for all the species and for all the statistical parameters results in a total global rank of 594 for the simulation based on MM5 meteorology and 598 for the simulation based on ECHAM4-OPYC3 meteorology. The overall performance of the model setup with climatic weather as input to the DEHM model performs equally well as the known and well-performing MM5 DEHM model setup with respect to analysis of monthly mean values over this ten-year period.

The fact that a climate model in a ten-year average predicts the weather just as correct as a weather forecast model with respect to monthly mean values and seasonal variability if the data are used in a chemical transport model is a major finding with respect to the research field of climate change impact on air pollution. It confirms the hypothesis stated in this experiment: The Atmosphere-Ocean General Circulation Model ECHAM4-OPYC3 is able to provide a realistic and consistent picture of the meteorological key parameters applied in the air pollution model.

5.2 Test for systematic errors

Since the climate model (ECHAM4-OPYC3) has a much lower resolution and in some cases simpler parameterizations, a systematic error in the air pollution results originating from the meteorology could be introduced. The follow-

ing analysis is carried out in order to test for any systematic biases of the results from the ECHAM4-OPYC3 based simulation relative to the results of the MM5 based simulation (see Sect. 4.2).

From Table 2 it can be seen that there is a systematic bias between the results based on the MM5 meteorology and the results based on ECHAM4-OPYC3 meteorology. The results of the MM5 based simulation generally predicts larger concentrations of the individual chemical species compared to the results of the ECHAM4-OPYC3 simulation. For most of the species (all except NH_3, HNO_3, O_3 and the wet deposition of SO_4^{2-}) this bias is tested to be significant beyond a significance level of 10%. Whether the MM5 based simulation is overestimating the concentration of the individual chemical species or the ECHAM4-OPYC3 based simulation is underestimating relative to observations, can not be concluded from this analysis. However, from the analysis of the total ranking of the fractional bias for every year (not shown), it was found that the ECHAM4-OPYC3 model setup performs slightly better than the MM5 model setup with respect to the fractional bias. The ECHAM4-OPYC3 setup has 186 points vs the MM5 setup which has 216 points. This indicates that the MM5 setup is over-predicting the concentrations. Conversely the MM5 based simulation is much better in predicting the variability in the data.

The observed systematic bias between the two simulations must originate from the difference in meteorology between the two model setups, since everything else is similar in the two simulations.

5.3 T-test results for the periods 1990–1999, 2040–2049 and 2090–2099

Until now, the performance of the ECHAM4-OPYC3 model setup has been tested in the validation period 1990–1999 for the specific EMEP measuring stations. In this section the scenario results are tested, but only for results at the same EMEP measuring sites of Europe.

In Table 3 results of the t-test are displayed. The t-test is here used to test for any significant changes between the 1990s and 2040s, between the 1990s and 2090s and finally between the 2040s and 2090s. This test is performed to see, if the mean values of the concentrations or wet depositions of the individual chemical species are changing with changes in the climate predicted by the ECHAM4-OPYC3 simulation (all decades are simulated with preserved 1990 emissions). In Table 3 the first three columns show the calculated t-value, the significance level and the fractional bias when the annual mean values of the species in 1990s is tested against the annual mean values of the same species in the 2040s. The next three columns shows the same result but for the periods 1990s against the 2090s and finally the three last columns shows the result of the period 2040s vs 2090s. A significant level within 10% has been chosen as the threshold value for statistical significance. The wet deposition of NH_4^+, NO_3^- and SO_4^+ and the concentration of HNO_3 are all chemical species for which the annual mean values are different within a significance of 10% and for which changes are significant in all three periods. Similarly, NH_4^+, sum of NH, NO_3^-, SO_2 and SO_4^{2-} are species with mean values that are changing significantly in one or two of the periods.

The first important conclusion which can be drawn from the results of Table 3 is that the tendency (decrease or increase in concentration) for each chemical species found in the first half of the century are the same in the second half of the century. There are no significant changes which only happens in the beginning of the century. The chemical species which are changed, are either changed over the total period (increase/decrease between the 1990s and the 2090s) or only changed in the second half of the century. This makes it reasonable from now on only to analyse the 1990s against the 2090s and assume that the comparison of these two decades represents the changes during the whole century. Of course fluctuations in the evolution of the individual species and meteorological parameters are likely to have happened, however the results here indicate that the changes between the two decades represent the total change within the century as well. Therefore in the further analysis only the 1990s will be evaluated against the 2090s.

Table 2. The DEHM simulation with MM5 meteorology and real emissions is compared to the DEHM simulation with ECHAM4-OPYC3 meteorology and real emissions with the t-test method. The t-value, the significant level in % and the fractional bias (FB) is displayed for the 15 selected chemical species and for the precipitation. The fractional bias is in this case calculated as

$$FB = 2 \frac{\overline{MM5} - \overline{ECHAM}}{\overline{MM5} + \overline{ECHAM}} \tag{8}$$

Both the diurnal average (MEAN), the hourly average (HOUR) and the diurnal maximum (DM) concentration of ozone are included in this analysis, though only the diurnal average concentration has been discussed in the visual analysis in section 5.

Chemical specie	t-value	sig. level %	FB
NH_3	0.26	>50	6.0
NH_4^+	1.98	10	19.3
SUM NH	5.71	0.1	19.6
WD. NH_4^+	19.55	<0.1	59.5
precipitation	−5.29	0.1	−17.8
HNO_3	1.25	50	8.1
NO_3^-	3.48	1	24.1
SUM NO	6.42	0.1	20.2
WD. NO_3^-	18.54	≪0.1	64.7
NO_2	6.62	0.1	13.6
SO_2	2.40	5	42.6
SO_4^{2-}	1.91	10	27.8
WD. SO_4^{2-}	0.83	50	10.0
O_3	0.21	>50	4.9
O_3 HOUR	0.21	>50	4.9
O_3 DM	0.09	>50	22.2

Secondly from Table 3 it can be seen that both NH_4^+ and the sum of NH are increasing significantly. On the contrary the wet deposition of NH_4^+ is decreasing significantly. The same is the case for the sulphur-group. The concentration of SO_2 and SO_4^{2-} are increasing and the wet deposition of SO_4^{2-} are decreasing.

A decrease in precipitation would logically decrease the wet deposition and thereby increase the concentrations of the corresponding species in the air. In the fifth row of Table 3 the evolution of the precipitation is shown. The averaged precipitation level over the total number of EMEP stations is not changing significantly between the two decades. This means there are no predicted changes in the precipitation level which can explain the observed evolution in ammonium (NH_4^+) and nitrate (NO_3^-). However, as already mentioned not only the precipitation amount which is shown here is important for the wet deposition process, also timing of precipitation events relative to the periods of high concentration, frequency of the precipitation events and finally type of precipitation (drizzle, snow, light to heavy rain etc.) are crucial with respect to the amount of the wet deposition.

Table 3. Results from the DEHM simulation with ECHAM4-OPYC3 meteorology and preserved 1990 emissions for the 1990's, 2040's and the 2090's, are compared using the t-test method for changes in mean values. The t-value, the significance level in % and the fractional bias (FB) are displayed for the 15 selected chemical species and for the precipitation. Here the fractional bias FB is calculated as

$$FB = 2\frac{\overline{2040s} - \overline{1990s}}{\overline{2040s} + \overline{1990s}} \tag{9}$$

and so forth. The changes in wet deposition of NH_4^+, NO_3^- and SO_4^+ and the concentration of HNO_3 are significant in all three tests. The changes in concentration of NH_4^+, sum of NH, NO_3^-, SO_2 and SO_4^{2-} are significant in one or two out of three tests. Here the accepted significant level is chosen to be within 10%. The fractional bias is defined so a positive values denotes an increase and a negative value a decrease.

	1990 t-value	vs. sig. level %	2040 FB %	1990 t-value	vs. sig. level %	2090 FB %	2040 t-value	vs. sig. level %	2090 FB %
NH_3	−0.08	>50	−1.5	−0.14	>50	−2.8	−0.07	>50	−1.4
NH_4^+	0.95	50	3.7	2.58	2	9.1	2.02	10	5.4
SUM NH	0.75	50	3.5	1.75	10	6.9	0.77	50	3.4
WD. NH_4^+	−2.78	2	−6.0	−5.19	0.1	−14.3	−3.12	1	−8.4
PREC	−0.08	>50	−0.3	0.69	50	2.2	0.81	50	2.5
HNO_3	3.04	1	10.1	7.09	0.1	24.9	4.70	0.1	14.9
NO_3^-	−0.54	>50	−2.2	−2.00	10	−7.6	−1.41	20	−5.4
SUM NO	0.54	>50	2.2	1.60	20	5.6	0.90	50	3.4
WD. NO_3^-	−2.51	5	−4.2	−4.01	0.1	−8.5	−1.91	10	−4.3
NO_2	−0.24	>50	−0.9	−1.06	50	−4.0	−0.85	50	−3.1
SO_2	1.04	50	3.8	2.14	5	7.9	1.42	20	4.1
SO_4^{2-}	1.16	50	5.6	3.34	1	14.0	2.73	2	8.4
WD. SO_4^+	−3.24	1	−5.4	−7.36	0.1	−12.2	−3.18	1	−6.9
O_3 MEAN	0.28	>50	6.5	0.65	>50	15.5	0.38	>50	9.0
O_3 HOUR	0.27	>50	6.4	0.65	>50	15.4	0.38	>50	9.1
O_3 DM	0.29	>50	6.9	0.69	50	16.4	0.40	>50	9.5

Finally the concentration and wet deposition of NO_3^- is evolving differently. Here the concentration of NO_3^- is decreasing at the same time as the wet deposition of the nitrate is decreasing. However, the observed decrease in nitrate is only significant in the total period 1990's vs. 2090's and the significance level is exactly 10% (just at the limit for significance by the definitions of this investigation).

5.4 Summary and discussion of the validation

Relative to observations the ECHAM4-OPYC3 model setup performs excellent with respect to the annual mean values of the different concentrations and wet depositions. However, the ECHAM4-OPYC3 setup fails to predict the variability in the data as expected. The correlation coefficients relative to observations are very low for most of the species. The ECHAM4-OPYC3 setup is able to predict a general decrease in SO_2 during the 1990s. This is not surprising since it originates from the reduced emissions and not the weather. Generally the concentration of particles and the wet depositions are predicted very well with respect to their mean values. However, the ECHAM4-OPYC3 setup have a tendency of underestimating the NO_3^- concentration when high con-

centration events occur (not shown). Also, for both model setups an underestimation of NO_2 is seen, probably due to the low resolution of the model.

O_3 is predicted very well both with respect to mean value and variability. This feature may result from a relatively low dependency of the weather relative to the dependency of the natural and anthropogenic emissions of NO_2 precursors and of the seasonal changes of global radiation and temperature.

The MM5 model setup is known to perform well and the ranking carried out here shows that the performance of the ECHAM4-OPYC3 setup are similar with respect to monthly and annual values. The ECHAM4-OPYC3 performs better with respect to mean values than the MM5 setup. However, it is the other way around in the case of prediction of the variability of the data.

A systematic bias for some species between the two different setups has been identified, which inherently must originate from the meteorology which is the only thing that differs between the two simulations. Furthermore from the analysis of the future scenario results it is concluded that it is reasonable only to include the 1990s and the 2090s in the further analysis, since the trends are the same in both half of the century.

Finally there is a tendency of an increase in the secondary particles concentrations (e.g. SO_4^{2-}) and a tendency of a decrease in the wet deposition of the same particles. The precipitation amount seems to remain unchanged in the investigated period. It is very important to remember that all these result are based on the location of the EMEP measuring sites in Europe and there is a risk that these locations might not represent the actual pollution or precipitation distribution of Europe. However, by assuming that these EMEP stations do represent the pollution distribution of Europe leads to the conclusion that the precipitation timing, frequency or type have changed between the two decades in order to explain the observed changes in particle concentration and the ancillary wet depositions.

Since the DEHM model is a hemispherical model, it is possible to analyse the changes between the two decades (1990s and 2090s) in every grid cell for the entire hemisphere. This will give a more adequate picture of the projections found in this study. In the following section, this full data set is analysed.

6 Scenario results and discussion

In this paper only a limited number of the 63 species included in DEHM will be displayed and discussed. For further details see Hedegaard (2007). The chosen species are sulphur dioxide (SO_2), sulphate (SO_4^{2-}), ozone (O_3), nitrogen dioxide (NO_2), hydroxyl radicals (OH) and isoprene (C_5H_8). Furthermore, some meteorological parameters important for the air pollution levels are displayed as well.

The results in this section are displayed with one figure for each parameter. Each of these figures contains four subplots. In the two upper plots, ten-year average values are shown for the two decades under study (1990s and 2090s). These ten-year average values are calculated from ten annual either accumulated or averaged values, depending on the characteristics of the actual parameter. For example the precipitation and the deposition is accumulated over each individual year before making a ten-year average, whereas e.g. temperature is first averaged over each year and afterwards averaged over the ten-year period to give a ten-year mean value. In the lower left subplot the difference between the two decades are shown. This difference is calculated both as an absolute difference and as a percentage difference. However, for each of the parameters only one of these two differences has been selected for illustration since they basically shows the same and it varies which of the difference plot are most visually illustrative.

In order to separate out insignificant low-level changes or to avoid noise where the 1990s mean values is close to zero, a white color is used to mark these uninteresting areas. Mean values below 1% of the maximum mean value in the 1990s is colored white in both types of the difference plot (except for the case of SO_2 in Fig. 7 and isoprene in Fig. 14 where

the threshold value is set to 1‰ of the maximum mean value of the 1990's).

Finally the lower right subplot of the figures shows the statistical significance of the change of mean values between the two decades. This significance is derived from the students t-test as in the previous sections. The legend of the plot is constructed so that all colors besides white marks the areas of significant changes within different significance levels. Here the threshold value for significance is chosen to be within the 0.95 fractile corresponding to the 10% significance level and a t-value of 1.737.

6.1 Meteorology

In Fig. 4 the precipitation from the ECHAM4-OPYC3 simulation is plotted. It is clear that the precipitation amounts in the Arctic regions will increase in the future. At the same time southern Europe and the south-western United States will become drier. In the analysis solely based on the EMEP observation station network, it was found that there was no significant chance in the EMEP area. However, with the results presented here it becomes clear that the northern increase and southern decrease in Europe in precipitation levels averages out, when solely comparing data extracted at the locations of the EMEP measuring network.

The lowest right plot of Fig. 4 shows that the overall changes in precipitation amount between the two decades are significant by the definition of significance given above. The reddish colors represent the areas with significant increase and the green colors represent significant decreases. Also here the fact mentioned above that the changes in the EMEP area average out becomes clear. The area where the most EMEP stations are located is not significant with respect to changes in precipitation levels in the next century and the rest of the EMEP stations, which lies within the changing areas, are divided between significantly increasing and decreasing areas.

It is noteworthy that the increase in the Arctic region is highly significant. Over large areas the significance level is within 0.1%, which is extremely significant. The same thing is valid for southern Europe, Caribbean, Mexico, California and a large maritime area close to the Hawaiian islands. However, here the significance values are negative, which means that the precipitation amount is decreasing in these areas during the next century.

In Fig. 5 the 2 m temperature (T2) is shown. Concerning the difference plot (lower left plot of Fig. 5), it is important to note that the color-scale is changed, so all colors are positive. In other words the temperature is increasing everywhere. Also the significance plot emphasizes this fact by showing extremely positive significance everywhere. This general temperature increase with local hot spots over Southern Europe and the Arctic is similar to other model results (Stendel et al., 2002).
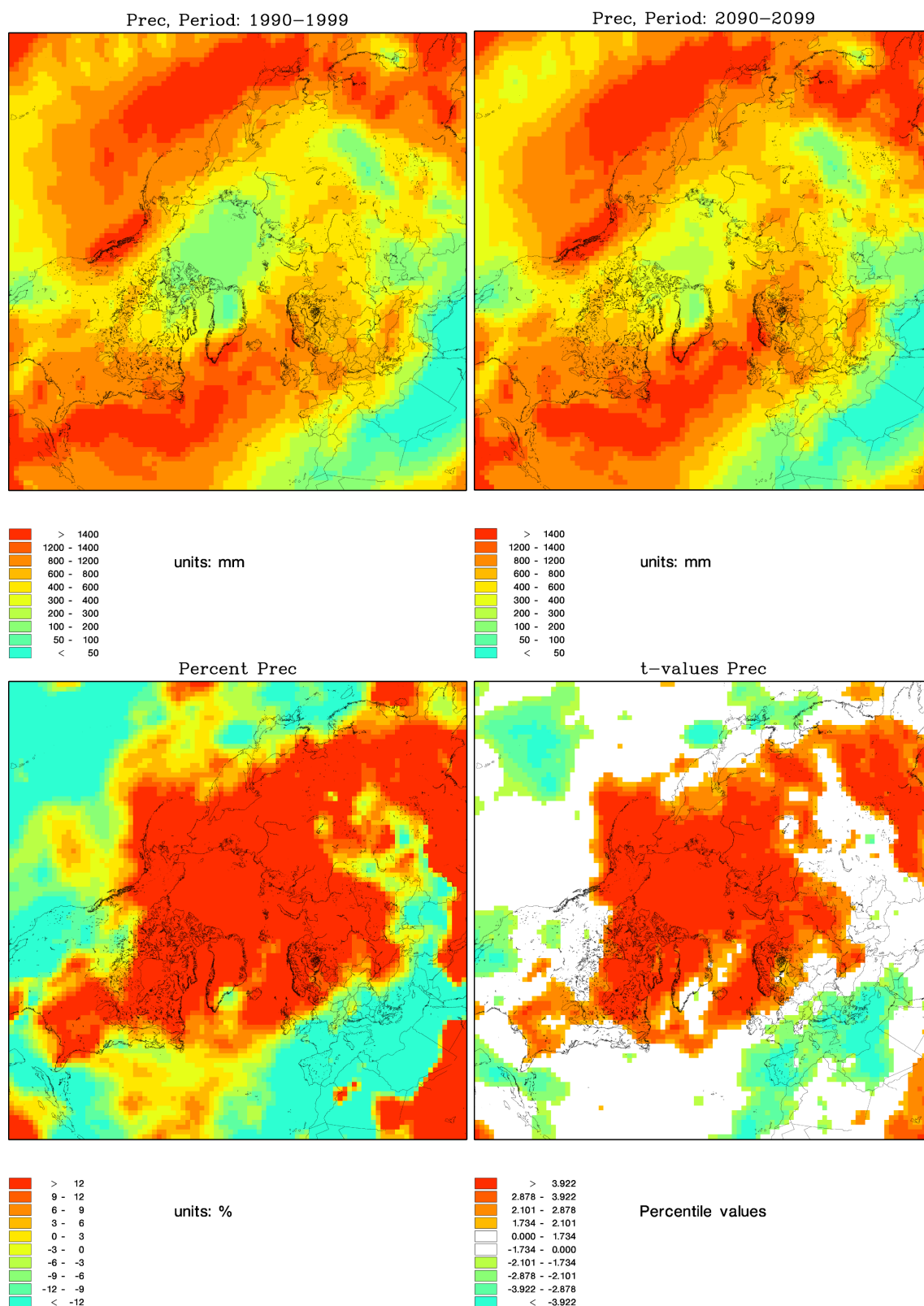
Fig. 4. The annual accumulated precipitation amount. In the upper left subplot the accumulated annual averaged precipitation amount is shown for the decade 1990–1999. The upper right subplot illustrates the same accumulated precipitation but for the decade 2090–2099. In the lower left subplot the difference between the two decades are shown in percent and finally the lower right subplot illustrates the significance level of the differences found in the former subplot according to the t-statistics.

Figure 6 shows the specific humidity. As in the previous figures, the lower left plot of the figure illustrates the difference between the 1990s and the 2090s. The color scale for this difference plot is changed so all colors represent an increase. The specific humidity increases everywhere. However, the increase is largest over the southern maritime regions. In Fig. 5 it was shown that the temperature increases everywhere in the domain of interest. When air temperature increases, the ability of the air to contain water becomes larger. Over the maritime areas more water will evaporate than over terrestrial areas and therefore a homogenous temperature increase can lead to an differentiated humidity increase pattern, with largest enhancement over sea (see e.g. over the Mediterranean sea in Fig. 6).

From the lower right plot of Fig. 6 it is clear that just like the temperature increase, the increase in the specific humidity is highly significant everywhere in the northern hemisphere (except over a small area in the Rocky Mountains).

6.2 Changes in air pollution levels calculated by DEHM

6.2.1 Sulphur dioxide

In Fig. 7 the impacts of climate change on the concentrations of sulphur dioxide (SO_2) are shown. SO_2 is a relatively short-lived species (a few days to a few weeks in the atmosphere) and for this reason the concentrations of SO_2 are largest close to the sources. SO_2 emissions are mainly due to burning of fossil fuels (coal, diesel etc.). These features are very clear in the two concentrations plot of Fig. 7. Here the largest concentrations of SO_2 are found close to the industrial areas which often coincide with the most dense populated areas. For example central Europe, eastern Asia and eastern United States are all areas of very high concentrations of SO_2. In Russia there are several hot spots of areas with high concentration of SO_2, which not necessarily coincide with the large cities. The Arctic situated city, Norilsk, is an example of this. Norilsk is a city in the Arctic part of Russia, which existence solely is based on the industrial extraction of nickel, copper, palladium, platinum etc. The city houses 300 000 people, who works with this metal production. The emission of SO_2 in Norilsk is approximately 2000 kton/year (AMAP, 2006)and therefore it is not surprising that the SO_2 signal of Norilsk is very clear in the hemispheric concentration plots (Fig. 7).

Over the Pacific and the Atlantic Ocean some lines of high SO_2 concentrations appear. These lines are the international routes of ships (diesel emitters). Since SO_2 is relatively short-lived, these very local maritime emissions, becomes evident in the concentration plots of SO_2 (Fig. 7).

Inspecting the figure reveals that the SO_2 concentrations are predicted to decrease significantly everywhere in Siberia in the next century. The largest increase in the SO_2 concentration is found over the populated areas (western United States, central and south Europe and eastern Asia). Here it

should be kept in mind that the emissions are kept constant at the 1990 level in this experiment, so the changes found here must be due to changes in the meteorological parameters. The SO_2 concentration from ship traffic seems to intensify a little both in the Atlantic and the Pacific Ocean in the future. Inspecting the significance plot of Fig. 7 (lower left) reveals that the observed enhancement is significant over both oceans. However, the changes in the Pacific are quite small and only visible because the threshold of 1% has been changed to 1‰ in this plot. Besides the ship routes, the areas of increasing SO_2 concentrations over western United States, central and southern Europe and eastern Asia are also highly significant.

6.2.2 Sulphate

In Fig. 8 the future evolution of sulphate (SO_4^{2-}) is shown. SO_4^{2-} is a secondary aerosol which is created from sulphur dioxide (SO_2). Whereas SO_2 is relatively short-lived, SO_4^{2-} on the other hand is dominated by long-range transport and therefore it is a very weather dependent parameter.

The concentration plots of Fig. 8 show that the concentration of SO_4^{2-} is small over the Pacific ocean and over the whole Arctic region. This indicates that even though SO_4^{2-} can be long-range transported, the regions of high SO_4^{2-} concentrations are situated relatively close to the main emission sources of SO_2.

It is interesting to note that the SO_4^{2-} concentration over Norilsk is predicted to increase significantly in the future decade due to climate change. Also over eastern United States and over a large area around and over southern Europe is the SO_4^{2-} concentration expected to increase. The fact that the SO_4^{2-} is predicted to increase can either be an expression of decreasing lifetime of SO_2 and therefore a higher production of SO_4^{2-} or an enhanced transport of SO_4^{2-} into these areas, since the emissions are kept constant in this experiment. A decrease in the lifetime of SO_2 is closely connected to an increase in O_3 through the chemical process described in Reaction (R1).

$$O_3 + h\nu \rightarrow O(^1D) + O_2$$
$$O(^1D) + H_2O \rightarrow 2OH$$
$$2OH + SO_2 \rightarrow SO_4 \tag{R1}$$
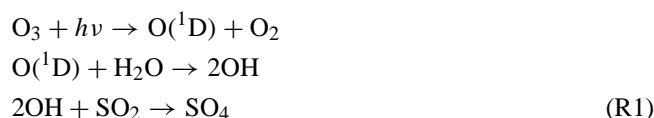
From Figs. 6 and 10 it can be seen that an increase in specific humidity and O_3 over the area of Norilsk is predicted, which makes the explanation above plausible. The increase in SO_4^{2-} concentration is seen as a very local phenomenon close to the source area of Norilsk. The surroundings of Norilsk is dominated by a significant decrease in SO_4^{2-} concentration.

In Fig. 9 the wet deposition of SO_4^{2-} is shown. The wet deposition of SO_4^{2-} is logically located at the same spots as
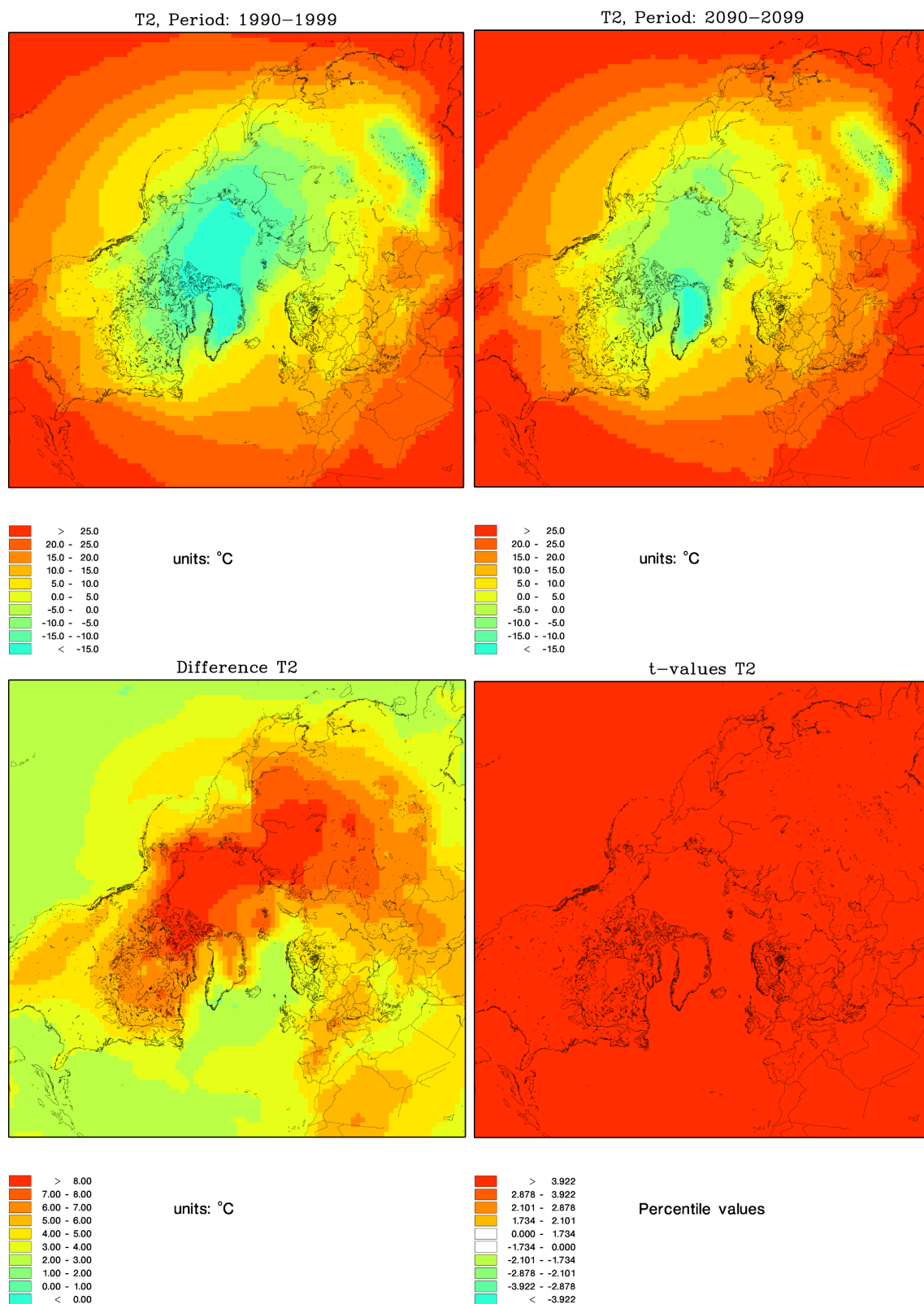
Fig. 5. 2 m temperature, as in Fig. 4, except the difference plot which in this case is shown as an absolute difference.
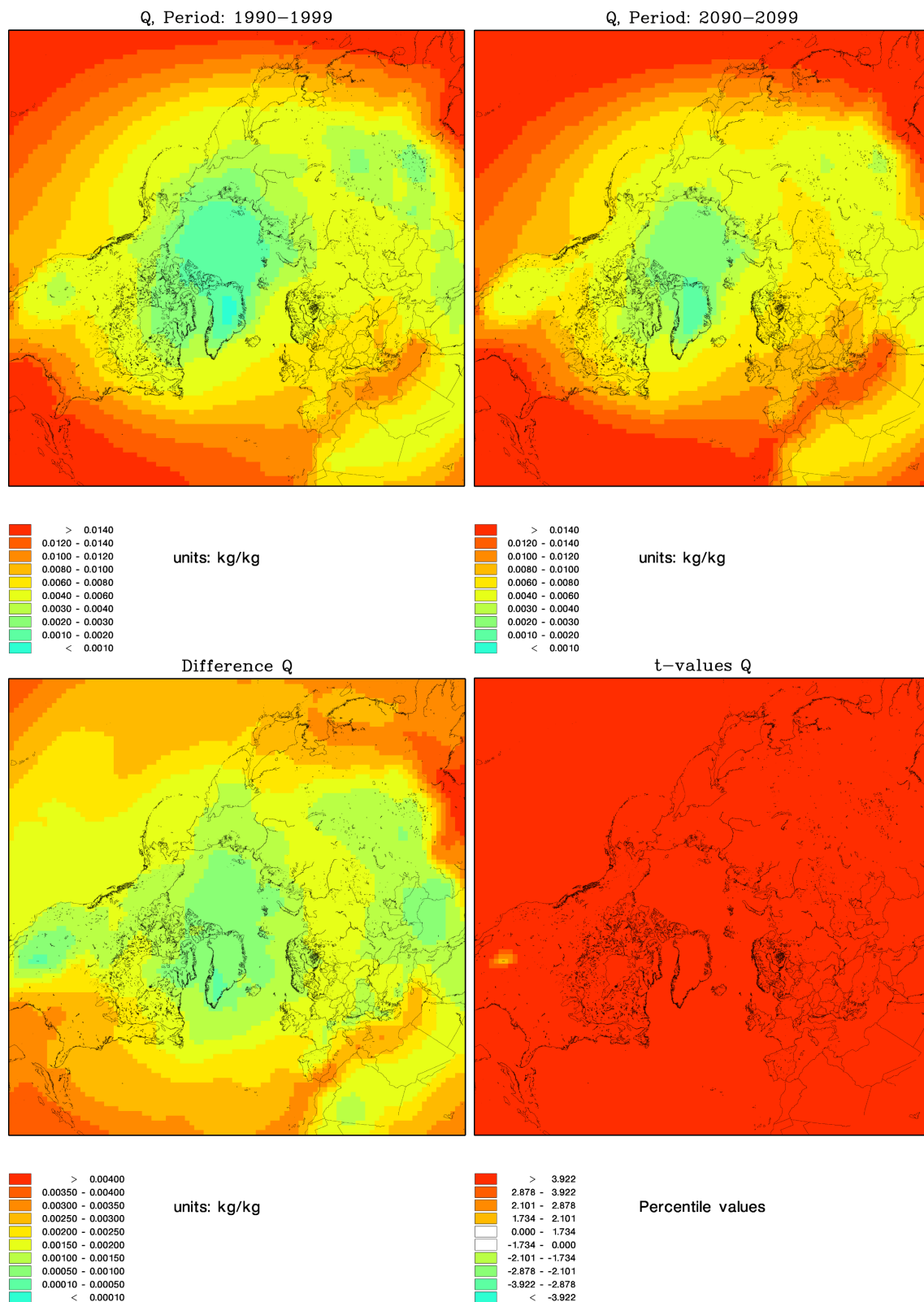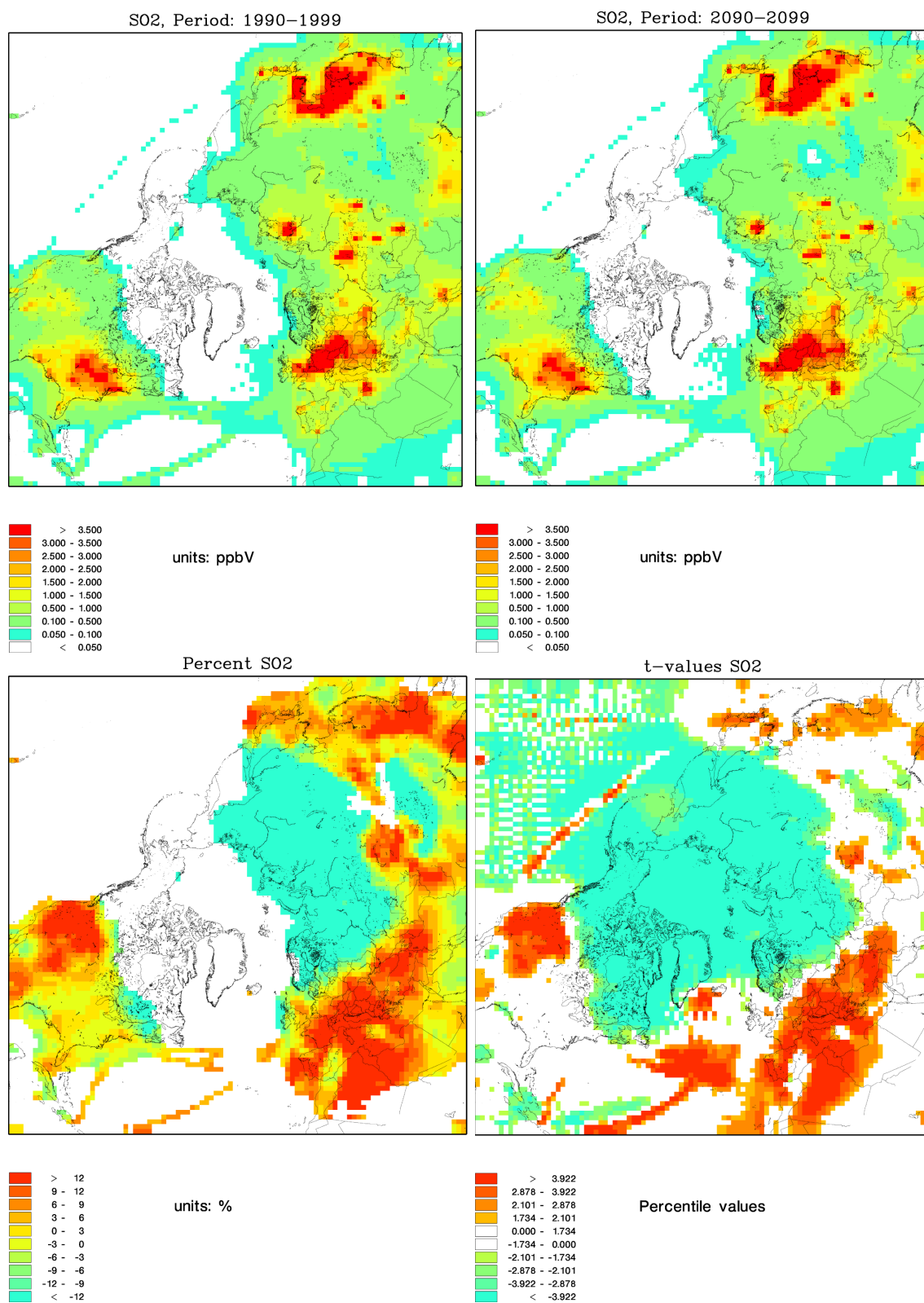
Fig. 6. As in Fig. 5 but for specific humidity.

Fig. 7. SO$_2$ concentration. In the upper left subplot the SO$_2$ mean concentration is shown for the decade 1990–1999. The upper right subplot illustrates the same mean concentration but for the decade 2090–2099. In the lower left subplot the difference between the two decades are shown in percent and finally the lower right subplot illustrates the significance level of the differences found in the former subplot according to the t-statistics.
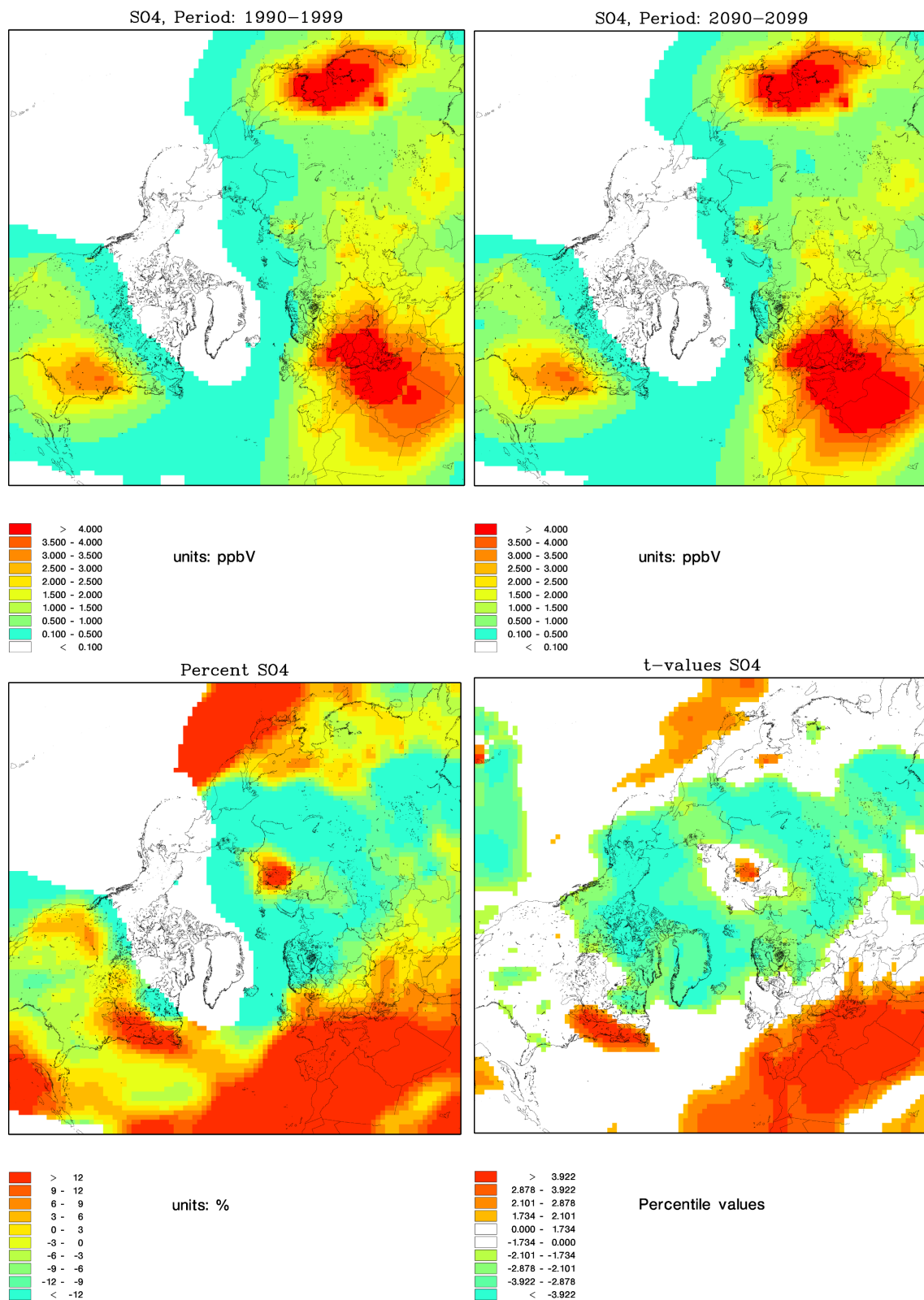
**Fig. 8.** SO_4^{2-} concentration, as in Fig. 7.

the areas of high concentrations of SO_4^{2-}. In some areas of the northern hemisphere the wet deposition is increasing and in other areas the wet deposition is decreasing in this model simulation. However, from the significance plot (lower right of Fig. 9) it is clear that none of these changes are significant. This can be explained from the characteristics of the precipitation. Precipitation is a highly intermittent on/off process, which in this statistical connection introduces a low signal-to-noise ratio.

6.2.3 Ozone

The impacts of climate change on the concentration of ozone (O_3) is displayed in Fig. 10. The areas of high O_3 concentrations are partly situated over the populated areas (cf. the upper plots of Fig. 10). However also a latitude dependent structure is evident in all four subplots of Fig. 10. In the difference plot (lower left plot) this structure is very clear. The O_3 concentration levels increase in the future and the increase is stronger with increasing latitude. North of approximately $30°$ N the increase is very significant, everywhere south of $30°$ N the difference in O_3 concentration changes and in the equatorial areas the O_3 concentrations levels tends to decrease significantly between the two decades. However, also a blurred land-ocean contrast in the O_3 increase is evident. The O_3 concentration generally increases less over the ocean.

6.2.4 Nitrogen dioxide

In Fig. 11 the concentration levels of nitrogen dioxide (NO_2) are shown. The emissions of NO and NO_2 originates mainly from traffic and power plants, which is also evident in the two concentration plots. Generally the NO_2 levels are decreasing where the O_3 levels are increasing and vice versa (see for example over Europe in Figs. 10 and 11). Also the Himalayan mountains is a good example of this inverse nature. Here a significant increase in NO_2 concentrations is detected in contrast to a decrease in the O_3 concentration and both these changes are significant. NO_2 and O_3 are linked through a chemical process (see Reaction R2). However, more investigations are needed to determine if new equilibria will occur under changed climate conditions between the involved chemical species.

$$NO + O_3 \rightarrow NO_2 + O_2$$
$$NO_2 + h\nu \rightarrow NO + O$$
$$O + O_2 \rightarrow O_3 \qquad\qquad\qquad\qquad (R2)$$
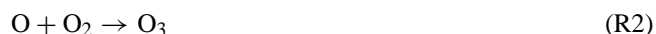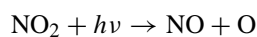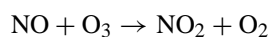
Only the Caribbean differs from this inverse structure. Here both O_3 and NO_2 are increasing significantly. In this case an explanation must be found elsewhere.

6.2.5 Hydroxyl radicals

In Fig. 13 the prediction of the concentration of hydroxyl radicals (OH) in the fifth layer (height approximately 230 m above the surface of the DEHM simulation are shown. The general lifetime for the OH radical is less than one second McGuffie and Henderson-Sellers (2001). Due to this very low existence time of OH, it is very difficult to evaluate the predicted concentrations with respect to measurements or prognostic statements. Furthermore a long-range transport model with a coarse resolution is not expected to simulate the real OH concentrations. However, in the DEHM model the lifetime of a great number of chemical species is dependent on the amount of OH radicals present. For this reason the changes in the concentration of OH can give some important information in the analysis of many other chemical species and their transformations. Also in the DEHM model the existence of OH radicals are instantaneously, since the model do not posses any memory of this specie, but is only estimated via a production term and a loss term.

Plotting the OH concentration at the surface (Fig. 12) it is clear that the OH concentration in the surface layer is predicted to increase over the maritime areas in contrast to the terrestrial areas where the OH concentration is predicted to decrease during the next century. Comparing the surface layer OH concentration (12) with the concentration from approximately 230 m altitude (Fig. 13) reveals some differences. Most important is this land-ocean contrast seen at the surface, which higher up in the atmosphere gets more blurred. The general decrease in the OH concentration over land is less pronounced in Fig. 13 compared to the surface layer Fig. 12.

6.2.6 Isoprene

Figure 14 shows the prediction of the Volatile Organic Compound (VOC) isoprene. Isoprene is included in the DEHM model from biogenic sources and is through participation in chemical reactions with OH acting as a sink for OH which explains the low OH concentration over land in the surface layer. The two upper plots of Fig. 14 show that isoprene primarily exists over land. From the absolute difference (lower left plot 14) it is clear that the biogenic emission of isoprene is expected to increase everywhere, where there are emitters available and this increase results in an increase in the concentrations which is highly significant. This feature is not surprising, since it is already observed that the temperature will increase by this model prediction. The emission of isoprene is a function of temperature, because the size of the emission is highly dependent on the growth of emitting plants.
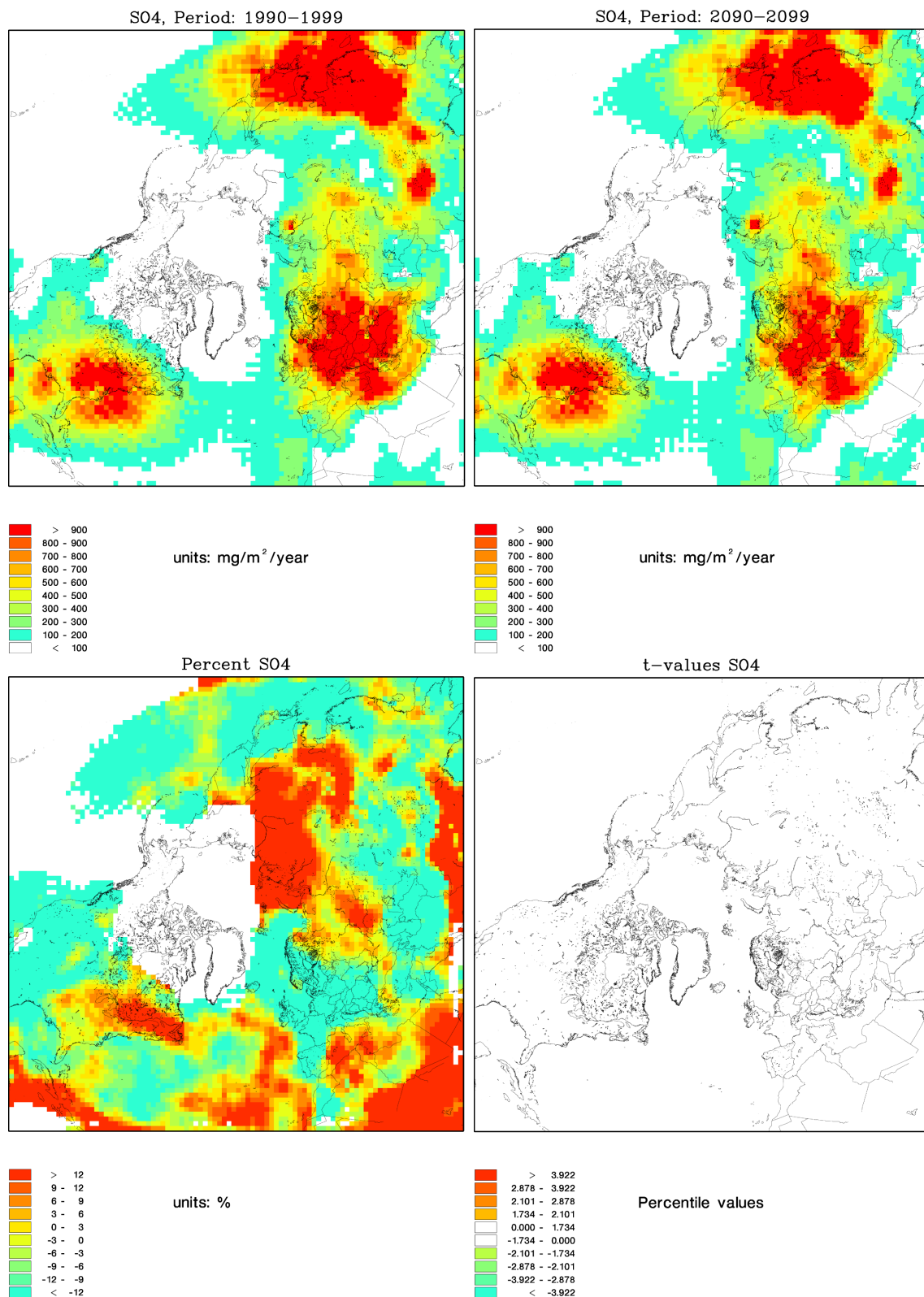
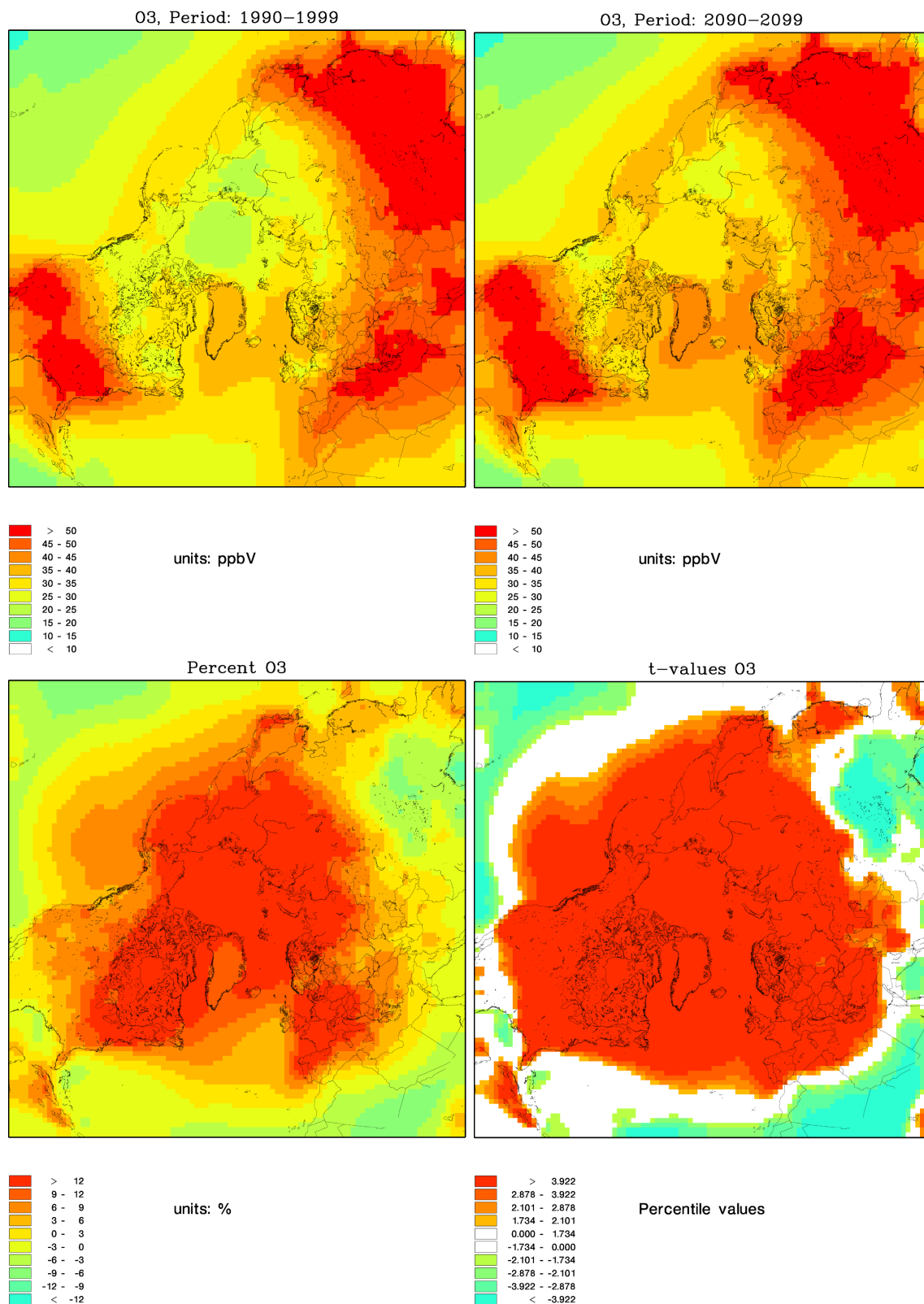**Fig. 9.** SO_4^{2-} wet deposition, as in Fig. 7.
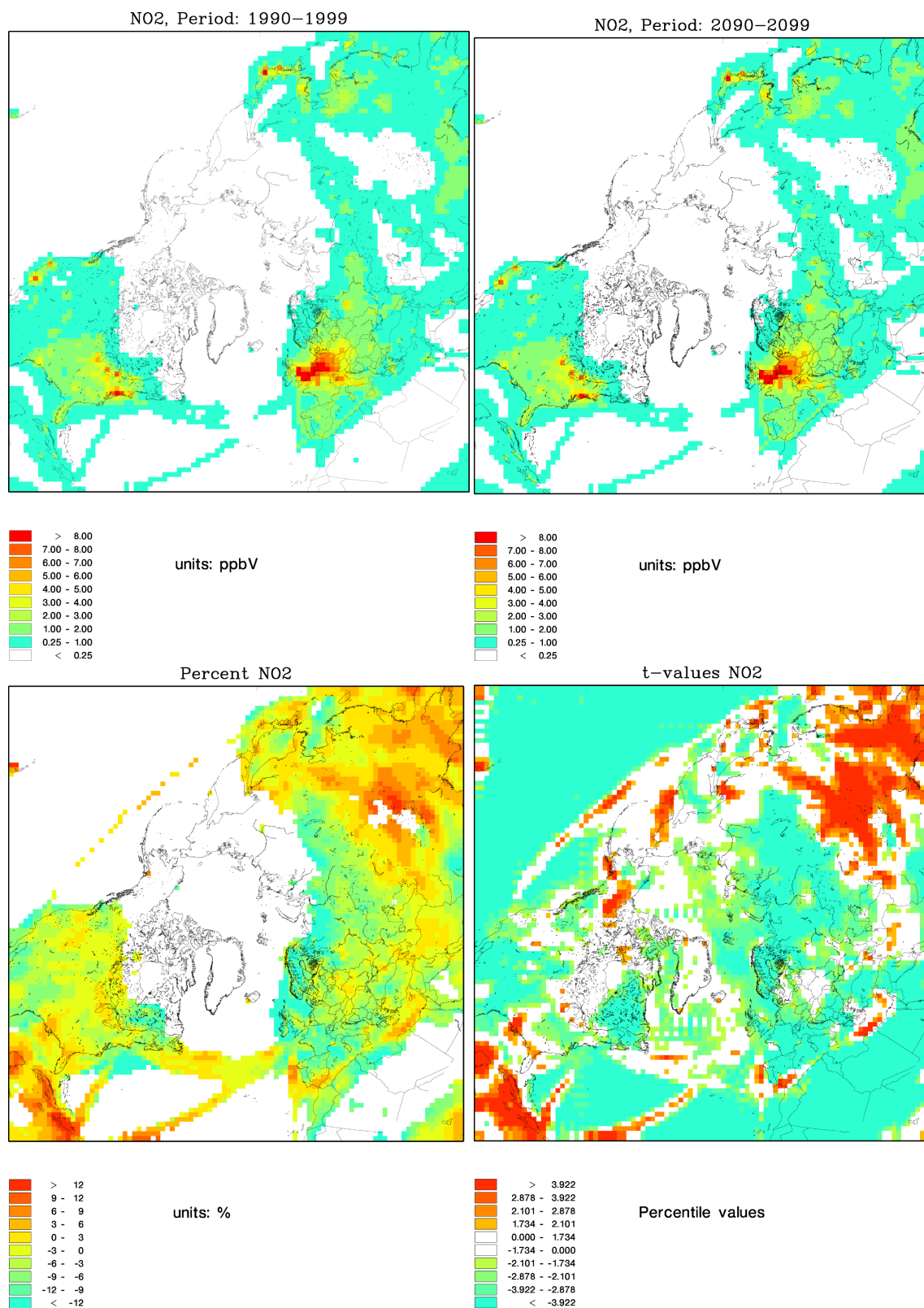
Fig. 10. O$_3$, as in Fig. 7.
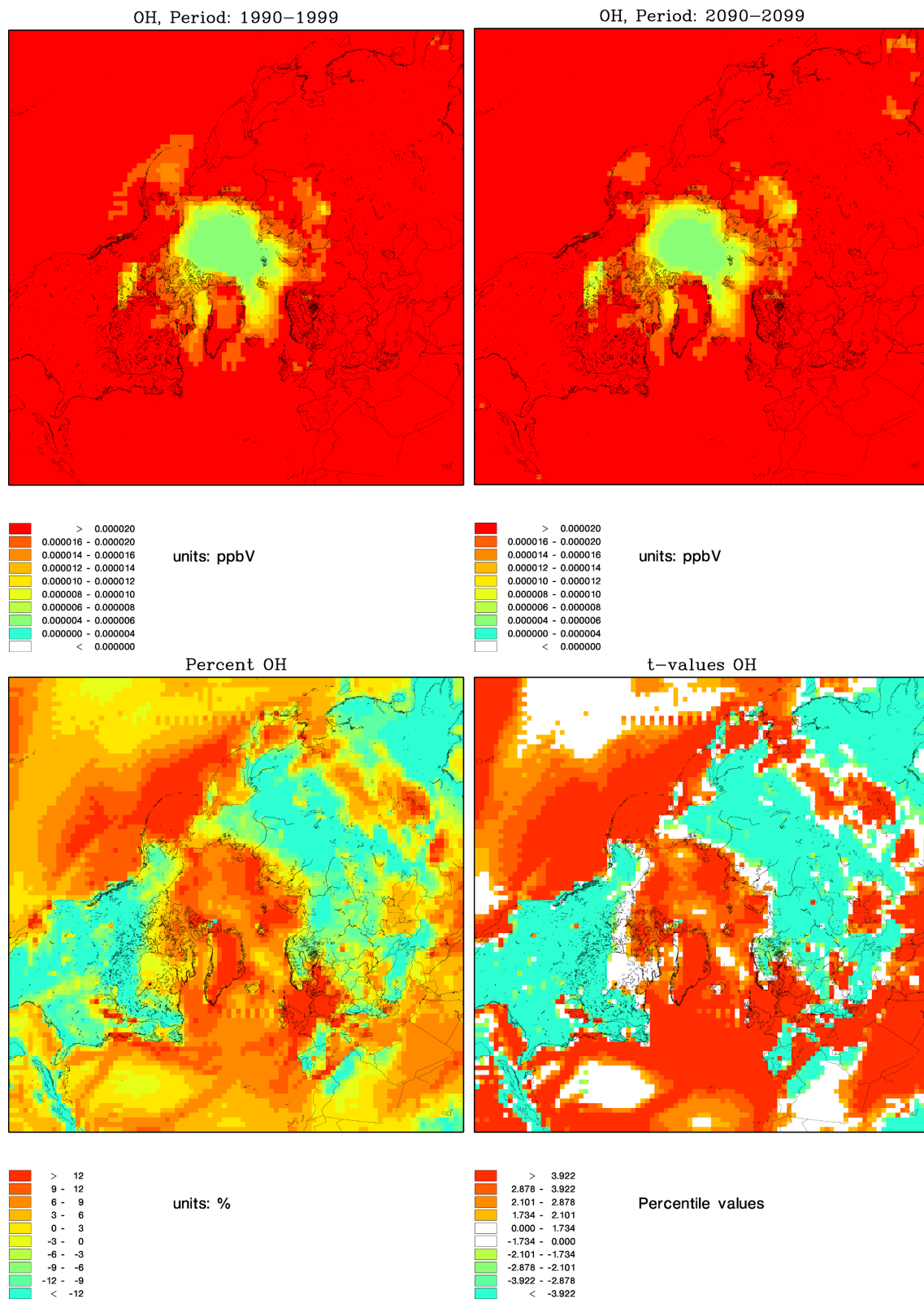
Fig. 11. NO$_2$, as in Fig. 7.
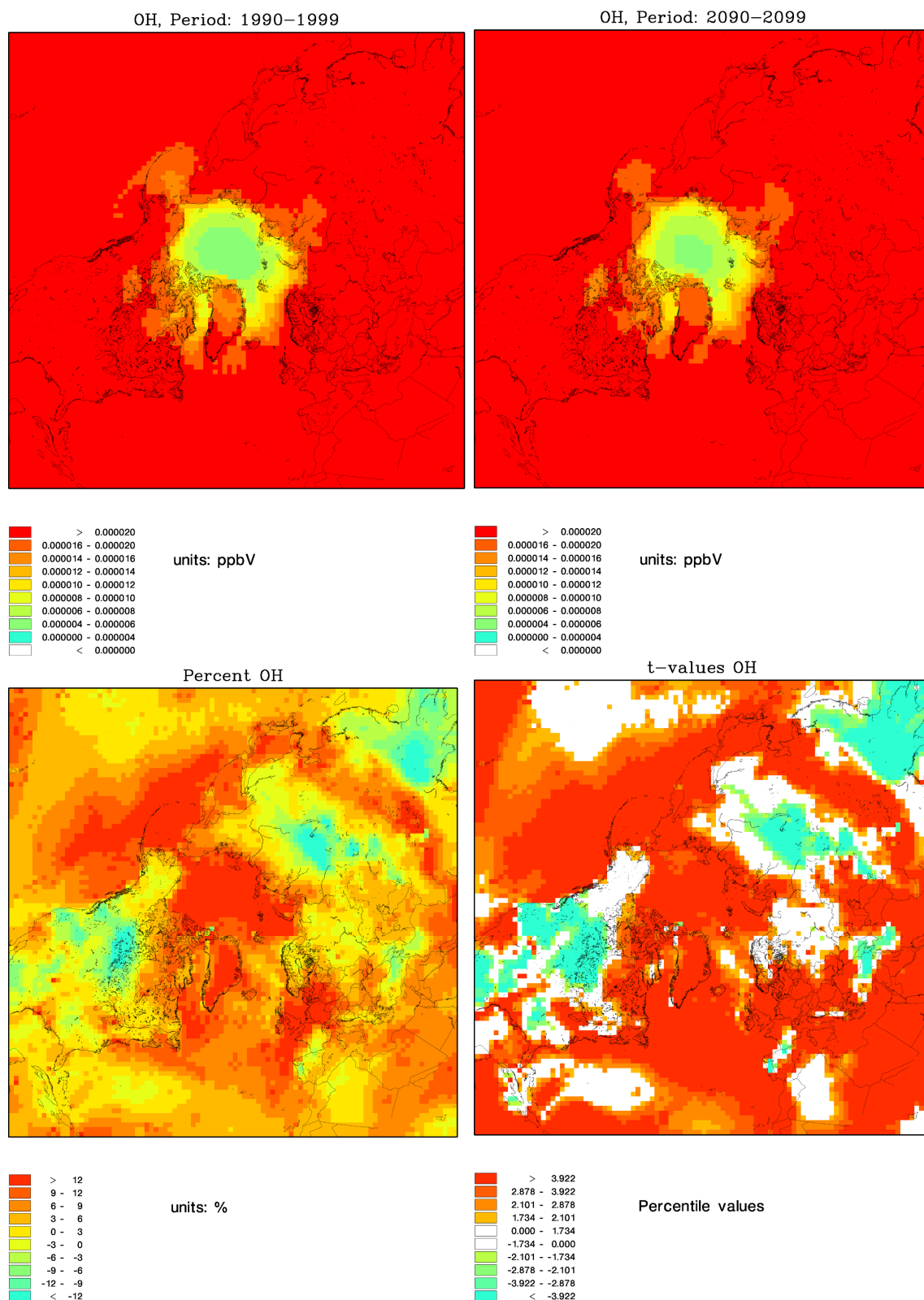
Fig. 12. OH layer 1, as in Fig. 7.
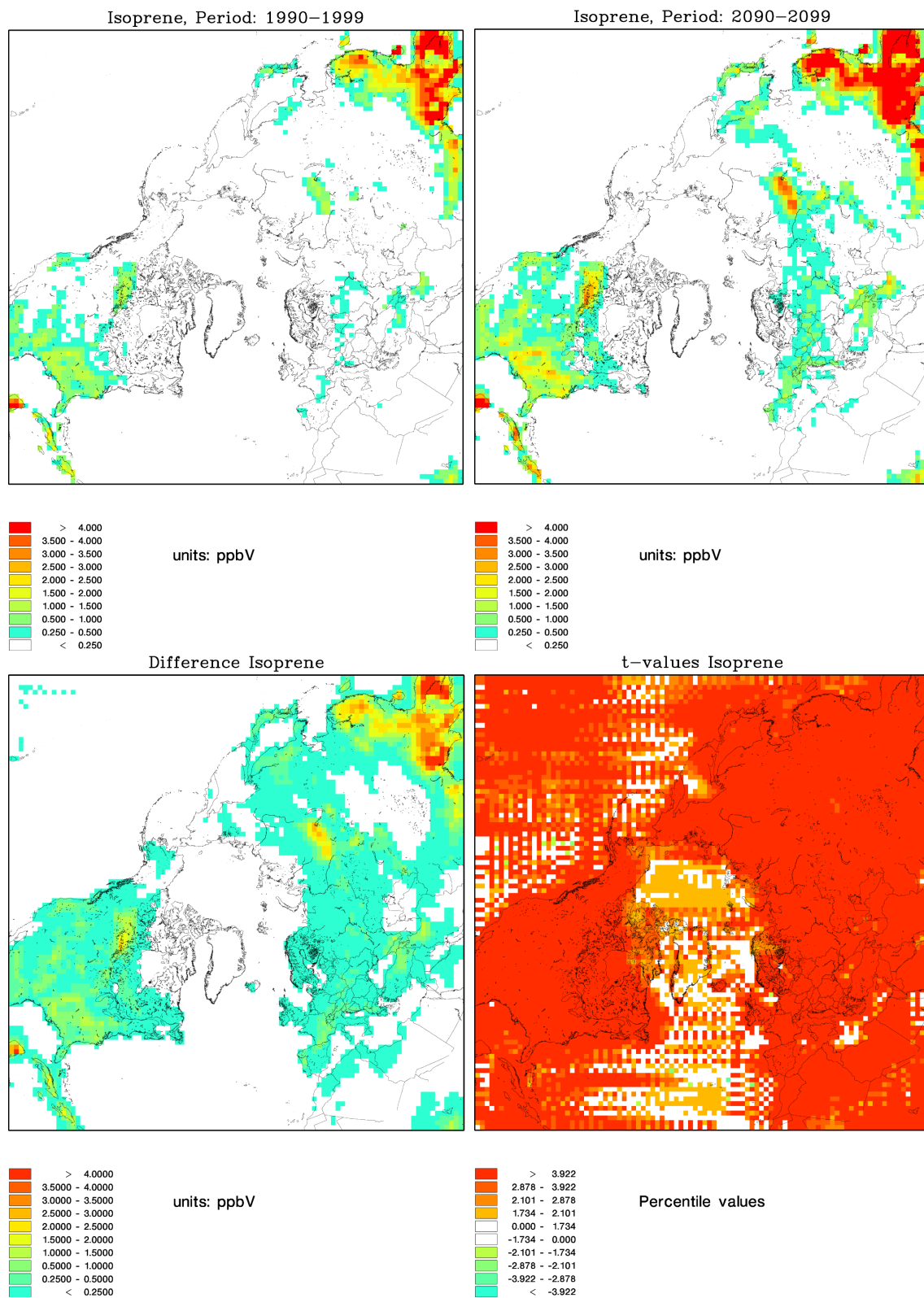
Fig. 13. OH layer 5, as in Fig. 7.

Fig. 14. Isoprene, as in Fig. 7, except for the difference plot which is shown as an absolute difference.

6.3 Discussion

One of the most pronounced changes in meteorology predicted by the ECHAM4-OPYC3 simulation is the global temperature increase. The temperature is predicted to increase everywhere in the Northern Hemisphere. However, the temperature increase enhances towards the North Pole.

From the DEHM simulation it was found that also the O_3 concentration is increasing everywhere North of approximately 30° N. The O_3 production is very dependent on the presence of the precursors NO_x and VOC's. In this experiment the anthropogenic emissions are kept constant. However, VOC's also have biogenic emitters, which can alter their emissions due to changes in meteorology in this experiment. The only natural VOC emitter included in the DEHM model is isoprene and it was found that isoprene increases everywhere over land due to the temperature increase and this can explain the predicted increase in O_3.

From Fig. 6 it was found that the specific humidity was increasing in the whole model domain. Increasing temperature results in an increasing humidity and thereby in an increasing number of H_2O molecules in the atmosphere if water is not a limiting factor. When O_3 already is present, more H_2O molecules will lead to more OH through the process shown in the Reaction (R3) below

$$O_3 + h\nu \rightarrow O_2 + O$$
$$O + H_2O \rightarrow 2OH \tag{R3}$$

An increase in temperature, specific humidity and O_3 concentration (only north of approximately 30° N) was found in the 21st century. By the reaction scheme R3 these projected increases must lead to an increase in the number of OH radicals. In Figs. 12 and 13 the concentration of these OH radicals is shown. The predicted increase by the reasoning above is confirmed from the concentration plots of Fig. 13. However, in the difference plot of Figs. 12 and 13 it becomes evident that the OH concentrations in the surface layer are increasing over sea and decreasing over land. In connection to the discussion above, it is easy to jump to the conclusion that the future temperature increase leads to an enhanced humidity increase over the maritime areas, which again results in more OH due to more water molecules. However, inspecting the plot of the predicted specific humidity reveals that the increase in humidity is much more latitudinal dependent and there are no similarities between the specific humidity figure and the OH concentration predictions.

This finding of a very sharp discontinuity between the terrestrial and the maritime concentration of OH leads to the possible connection of the isoprene concentration (see Fig. 14). As mentioned earlier, isoprene emissions are only present over land and the concentration of isoprene is confined to the source areas, because of a very short chemical lifetime. The Reaction (R4) below reveals that isoprene consumes OH. In the DEHM model this is the only chemical

reaction included, where OH radicals are removed from the atmosphere by isoprene. Besides isoprene a great number of other chemical species reacts with OH and remove it from the atmosphere. However, the observed concentration of isoprene over land (see Fig. reffig:isoprene) seems to be the dominating OH-sink in this experiment near the land surface.

$$C_5H_8 + OH + O_2 \rightarrow OHC_5H_8O_2 \tag{R4}$$

Since OH is a very important agent for a great number of chemical reactions, an increase in the number of OH must necessarily lead to an increase in the number of chemical reactions taking place and this will have a great influence on the lifetimes of many chemical species. As an example the lifetime of NO_2 will be reduced and lead to an increased level in NO_3^- and nitric acid (HNO_3).

Another interesting result of the analysis carried out here is the fact that the concentration of SO_4^{2-} increases over the Arctic metal industry city, Norilsk, even though the surroundings of Norilsk is characterized by a general decrease. The general predicted decrease in SO_4^{2-} concentration over Siberia can be explained by an increase in wet deposition due to an increase in precipitation over the area. In the lowest panel of Fig. 7 it is clear that the concentration level of SO_2 is significantly decreasing and SO_4^{2-} is significantly increasing over the city of Norilsk. This means that the increase in SO_4^{2-} concentration do not originate from an increase in the concentration of SO_2. However, since it is predicted that there will be more free OH radicals in the future, it could be concluded that more of the present SO_2 will transform into SO_4^{2-} and thereby increasing the SO_4^{2-} concentration and decreasing the SO_2 concentration in the future.

The natural emitted VOC, isoprene is a strong O_3 precursor. In Fig. 14 it was found that the isoprene concentrations were increasing everywhere over the terrestrial areas. Trees and bushes are typical isoprene emitters and therefore the emission of isoprene only takes place over land. The projected level of isoprene will alter the O_3 production in a positive direction and thereby enhancing the O_3 level.

Langner et al. (2005) used the regional chemistry/transport/deposition model MATCH to simulate the distribution of surface ozone in the future. They found a general increase in the surface O_3 concentration over southern and central Europe. Langner et al. (2005) calculated the domain-total emission of isoprene to increase with 59% due to the predicted temperature increase. This is generally consistent with the results found in the simulations described in this paper. However, Langner et al. (2005) also found a decrease in surface O_3 in northern Europe. In this study a smaller increase in surface O_3 over southern and central part of Scandinavia was predicted.

Langner et al. (2005) states that the predicted changes found in surface O_3 concentrations are substantial and if the climate scenario (IPCC, IS92a) used in their study is representative for the future climate, the increase in surface O_3

due to the predicted warming would be significant compared to the expected reductions resulting from the emission reduction protocols currently in force.

This is in line with Tuovinen et al. (2002) who have made a sensitivity analysis of which factors will effect the surface O_3 concentration in Europe. They found that the increased biogenic VOC emissions significantly will counteract the effects of reduced anthropogenic emissions.

Murazaki and Hess (2006) have also studied the contribution from climate change on the future O_3 levels and spatial distribution with the global chemical transport model MOZART-2. Substantially different from the simulations carried out here, Murazaki and Hess (2006) kept both the anthropogenic and biogenic emissions constant (personal e-mail correspondence with P. Hess, 2006). On the contrary only the anthropogenic emissions were kept constant in the simulations described in this paper. The concentration of isoprene is highly dependent on temperature in the parameterizations of isoprene in the DEHM model. Murazaki and Hess (2006) concludes: "Overall, the change in background ozone can be viewed as a competition between increased ozone production over high-emission regions combined with a shorter ozone lifetime in travel across remote regions. The net effect is a decrease in background level of ozone over the United States". Here Murazaki and Hess (2006) have divided the surface O_3 into two contributions; the local produced O_3 and the background O_3. In the high emission areas the local increase in O_3 is expected to exceed the decrease in background O_3 resulting in a net increase. On the contrary a net decrease in ozone are predicted away from these high-emission zones. In the work carried out here the O_3 concentration is predicted to increase all over the United States (cf. Fig. 10). This difference relative to results of Murazaki and Hess (2006) is probably due to the lack of the temperature dependent biogenic emissions in the experiment carried out by Murazaki and Hess (2006). These emitters are as earlier mentioned O_3 precursors and they contribute with a relatively large increase in O_3 concentration over land.

Johnson et al. (2001) found that the impact of climate change decreases the net production of O_3 with approximately $120\,Tg/yr$ in the troposphere. However, Johnson et al. (2001) did not include the climate change effect on the natural VOC emitters. In the DEHM model the process which Johnson et al. (2001) addresses the loss of ozone production to $(O(^1D)+H_2O \rightarrow 2OH)$ is included. This means that the results found here include both effects and the result is clear: The net O_3 production is predicted to increase in the future due to climate change.

7   Summary, conclusions and future perspectives

A three dimensional chemical long-range transport model has been used to simulate the changes in air pollution due to climate change in the three decades 1990s, 2040s and 2090s.

In order to separate out the effect from climate change, the anthropogenic emissions have been kept on a constant 1990 emission level. The input meteorology is provided by the atmosphere-ocean general circulation model ECHAM4-OPYC3, which has been forced with the IPCC A2 emission scenario. This model setup has been validated against simulations based on MM5 meteorology and against observations from the EMEP measuring network in Europe. The predicted results for the future decades has been evaluated with respect to meteorology and the levels and distributions of some important chemical species have been analysed.

In order to test the model performance several statistical evaluation methods have been applied. The climate model (ECHAM4-OPYC3) fails to predict the exact timing of the various meteorological parameters as expected and this feature is reflected in the output of the DEHM model. The precipitation in a climate model is statistical and therefore it cannot be expected of the ECHAM4-OPYC3 model to time e.g. the precipitation events correctly and this influences the resulting wet depositions and concentrations in the air. However, averaging over a long period this feature becomes insignificant.

The data from the test period has been evaluated with the ranking method. The ECHAM4-OPYC3 DEHM model setup predicts the annual mean level of most of the selected chemical species correctly and in many cases the simulation based on climatic weather suits the annual mean levels even better than the simulation based on weather forecast data (MM5 setup). In conclusion the overall performance of the results based on ECHAM4-OPYC3 meteorology has similar performance as the MM5 setup. Both model setups simulate the observational data acceptably well with respect to annual mean values and seasonal variation based on monthly mean values. The performance of the MM5 – DEHM is known to be good from earlier studies. Therefore it can be concluded that: Running a chemical long-range transport model on data from a climate model like the ECHAM4-OPYC3 is scientifically sound.

From analysis of the data of the three decades (1990s 2040s and 2090s) it was found that the trend for the selected chemical species is the same between all three decades, when evaluation solely takes place at the sites where the EMEP stations are present. It was therefore concluded that it is reasonable to discard the 2040s decade in the further analysis.

The Northern Hemisphere has been analysed with respect to meteorology and concentration, wet and dry deposition of some selected species. The predicted temperature increase throughout the 21st century was found to be the dominating impact factor in these studies. The temperature increase results in an increase in the biogenic emissions of isoprene. Isoprene is a strong ozone precursor and the O_3 production is projected to increase significantly in these simulations. This increase in O_3 together with an increase in specific humidity is found to enhance the reaction rates of a great number of chemical reactions. The humidity and O_3 increase results in

an increase in concentrations of OH, which are the activating agents in many chemical processes. For example an indication of an enhanced SO_2 to SO_4^{2-} conversion and decreased lifetimes of some primary species were found.

This study is only in the beginning of an accelerating research field with respect to the impacts of climate change on air pollution. From the work carried out here the main conclusions are that it is scientifically sound to run a chemical transport model on climate data and that the temperature increase predicted by a great number of climate models seems to have a dominating effect on the future air pollution levels and distributions. This study has created a wide range of new hypothesis, which will be very interesting to study and test in the future.

The experiment carried out here is based on climate data forced with the IPCC A2 scenario. It could be interesting to perform a whole range of simulations forced with the different IPCC emission scenarios. A study like this would create an understanding of the resulting variety of air pollution distributions and levels as a results of the impact of climate change due to the different scenarios.

In order to understand and quantify the effects on the different air pollutants from a single meteorological parameter, a large amount of sensitivity studies are needed. For example, it can be hypothesized that climate change will have a large influence on the typical atmospheric transport patterns. From this experiment it was found that the signal from a projected temperature increase and hence the change in biogenic emissions is so strong that the signal from e.g. a change in transport patterns has been difficult to distinguish from other important processes in the model results. Therefore, it is necessary in the future to carry out a great number of sensitivity studies where e.g. all parameters are kept constant except the parameter under examination. In this way it will be possible to test the effect of the meteorological parameters separately and hereby get an idea of the sign and size of the various effects.

The contribution from the biogenic VOC emitters due to the temperature increase are documented to be very significant. Currently the parametrization of the natural VOC emitters in the DEHM model is only including isoprene. Terpenes are another group of VOCs, which are known to be released from biogenic sources as a function of temperature. The temperature dependent natural VOC emissions are composed of many contributions. Isoprene is known to produce ozone in contrast to terpenes, which are acting as a loss term for ozone. Therefore a sophistication of the biogenic emissions module in the model is one of the aims in the future.

Finally the experiments carried out have been time-sliced in order to save computing time. In a future study it might be feasible to do the simulations in one continuous run in order to identify any possible fluctuations within the century. Another initiative could be to integrate data from a regional climate model like e.g. HIRHAM (Hesselbjerg Christensen et al., 1996) and thereby simulate one of the smaller but higher-resolution domains of DEHM by running it in nested mode. This regional experiment would result in having relatively high resolution data over a limited area like e.g. Europe.

There is no doubt that the ultimate challenge here will be a two-way coupling of the chemical transport model and the climate model. This would enable the air pollution impacts to feedback on the climate, thereby creating a much more realistic simulation of the total climate-air pollutant system. Furthermore it would be interesting to run the system with future emission reduction scenarios in order to quantify the impacts from climate change vs. the impacts from the anthropogenic emission reductions.

A huge number of suggestions for future work exist and there is no doubt that this branch of combined climate change and air pollution research will grow. This research will inherently contribute with decisive knowledge to the policy makers in the future.

Edited by: A. B. Guenther

References

AMAP: AMAP Assessment 2006: Acidifying Pollutants, Arctic Haze, and Acidification in the Arctic, Scientific report, AMAP, 2006.

Brandt, J.: Modelling Transport, Dispersion and Deposition of Passive Tracers from Accidental Releases, Ph.D. thesis, University of Copenhagen, National Environmental Research Institute and Risø National Laboratory, 1998.

Brandt, J., Bastrup-Birk, A., Christensen, J. H., Mikkelsen, T., Thykier-Nielsen, S., and Zlatev, Z.: Testing the importance of accurate meteorological input fields and parameterizations in atmospheric transport modelling, using DREAM - validation against ETEX-1, Atmos. Environ., 32, 4167–4186, 1998.

Brandt, J., Christensen, J. H., Frohn, L. M., and Berkowicz, R.: Operational air pollution forecasts from regional scale to urban street scale. Part 1: System description, Phys. Chem. Earth B, 26, 781–786, 2001a.

Brandt, J., Christensen, J. H., Frohn, L. M., and Berkowicz, R.: Operational air pollution forecasts from regional scale to urban street scale. Part 2: Performance Evaluation, Phys. Chem. Earth B, 26, 825–830, 2001b.

Brandt, J., Christensen, J. H., Frohn, L. M., Berkowicz, R., Skjøth, C., Geels, C., Hansen, K., Frydendall, J., Hedegaard, G., Hertel, O., Jensen, S., Hvidberg, M., Ketzel, M., Olesen, H., Løfstrøm, P., and Zlatev, Z.: THOR -an operational and integrated model system for air pollution forecasting and management from global to local scale, in: Proceedings from the First ACCENT Symposium, Urbino, Italy, p. 6, 2005.

Christensen, J. H.: Testing Advection Schemes in a Three-Dimensional Air Pollution Model, Mathematical and Computational Modelling, 18, 75–88, 1993.

Christensen, J. H.: Transport of Air Pollution in the Troposphere to the Arctic, Ph.D. thesis, Department of Environment and Research, NERI, 1995.

Christensen, J. H.: The Danish Eulerian Hemispheric Model - A three-dimensional air pollution model used for the Arctic, Atmos. Environ., 31, 4169–4191, 1997.

Christensen, J. H.: Prediction of Regional scenarios and Uncertainties for Defining EuropeaN Climate change Risk and Effects PRUDENCE, Tech. Rep. EVK2-ct2001-00132, Danish meteorological institute, 2005.

Frohn, L. M.: A study of long-term high-resolution air pollution modelling, Ph.D. thesis, University of Copenhagen and National Environmental Research Institute, 2004.

Frohn, L. M., Christensen, J. H., and Brandt, J.: Development and testing of numerical methods for two-way nested air pollution modelling, Phys. Chem. Earth, 27, 1487–1494, 2002a.

Frohn, L. M., Christensen, J. H., and Brandt, J.: Development of a High-Resolution Nested Air Pollution Model. The Numerical Approach, J. Comput. Phys., 179, 68–95, 2002b.

Frohn, L. M., Christensen, J. H., Brandt, J., Geels, C., and Hansen, K. M.: Validation of a 3-D hemispheric nested air pollution model, Atmos. Chem. Phys. Discuss., 3, 3543–3588, 2003, http://www.atmos-chem-phys-discuss.net/3/3543/2003/.

Geels, C., Brandt, J., Christensen, J. H., Frohn, L. M., Hansen, K. M., and Skjøth, C. A.: Long-term calculations with a comprehensive nested hemispheric air pollution transport model, in: Proceedings from the First ACCENT Symposium, NATO ARW workshop, Springer, Borovetz, Bulgaria, 185–196, 2004.

Graedel, T., Bates, T., Bouwman, A., Cunnold, D., Dignon, J., Fung, I., Jacob, D., Lamb, B., Logan, J., Marland, G., Middleton, P., Pacyna, J., Placet, M., and Veldt, C.: A compilation of inventories of emissions to the atmosphere, Global Biogeochem. Cy., 7, 1–26, 1993.

Grell, G., Dudhia, J., and Stauffer, D.: A Description of the Fifth-Generation Penn State/NCAR Mesoscale Model (MM5), NCAR Technical Note NCAR/TN-398+STR, Mesoscale and Microscale Meteorology Division, National Center for Atmospheric Research (NCAR), Boulder, Colorado, 122 pp., 1995.

Guenther, A., Hewitt, C., Erickson, D., Fall, R., Geron, C., Graedel, T., Harley, P., Klinger, L., Lerdau, M., McKay, W., Pierce, T., Scholes, B., Steinbrecher, R., Tallamraju, R., Taylor, J., and Zimmerman, P.: A Global-Model of Natural Volatile Organic-Compound Emissions, J. Geophys. Res., 100, 8873–8892, 1995.

Guenther, A., Karl, T., Harley, P., Wiedinmyer, C., Palmer, P., and Geron, C.: Estimates of global terrestrial emissions using MEGAN (Model of Emissions of Gases and Aerosols from Nature, Atmos. Chem. Phys., 6, 3181–3210, 2006, http://www.atmos-chem-phys.net/6/3181/2006/.

Hedegaard, G.: Impacts of climate change on air pollution levels in the Northern Hemisphere, Tecnical Report 240, National Environmental Research Institute, Aarhus University, Frederiksborgvej 399, P.O. Box 358, 4000 Roskilde, 2007.

Hesselbjerg Christensen, J., Christensen, O., Lopez, P., Meijgaard, E., and Botzet, M.: The HIRHAM4 Regional Atmospheric Climate Model, Scientific Report 96-4, Danish Meteorological Institute, Copenhagen, 1996.

Hjellbrekke, A.: EMEP Co-operative Programme for Monitoring and Evaluation of the Long-range Transmission of Air Pollutants in Europe, Data report 1998, part 1: Annual summaries, EMEP/CCC-Report 3, EMEP, 2000.

Johnson, C., Stevenson, D., Collins, W., and Derwent, R.: Role of climate feedback on methane and ozone studied with a coupled Ocean-Atmosphere-Chemistry model, Geophys. Res. Lett., 28, 1723–1726, 2001.

Langner, J., Bergstrøem, R., and Foltescu, V.: Impact of climate change on surface ozone and deposition of sulphur and nitrogen in Europe, Atmos. Environ., 1129–1141, 2005.

Malmberg, A.: Erlang S Statistiske tabeller, Vol. 5, G E C GAD København, 1985.

McGuffie, K. and Henderson-Sellers, A.: Forty years of numerical climate modelling, Int. J. Climatol., 21, 1067–1109, 2001.

Monson, R., Trahan, N., Rosenstiel, T., Veres, P., Moore, D., Wilkinson, M., Norby, R., Volder, A., Tjoelker, M., Briske, D., Karnosky, D., and Fall, R.: Isoprene emission from terrestrial ecosystems in response to global change: minding the gap between models and observations, Philos. T. R. Soc. A, 365, 1677–1695, 2007.

Mosca, S., Graziniani, G., Klug, W., Bellasio, R., and Bianconi, R.: ATMES-II Evaluation of Long-range dispersion models using 1st ETEX release data., 2. Draft report Vol. 1 and Vol. 2, ETEX Symposium on Long-range Atmospheric Transport, Model Verification and Emergency Response, Vienna, 1997.

Murazaki, K. and Hess, P.: How does climate change contribute to surface ozone change over the United States, J. Geophys. Res., 111, D05301, doi:1029/2005JD005873, 2006.

Nakicenovic, N., Alcamo, J., Davis, G., de Vries, B., Fenhann, J., Gaffin, S., Gregory, K., Grübler, A., Jung, T., Kram, T., Rovere, E. L., Michaelis, L., Mori, S., Morita, T., Pepper, W., Pitcher, H., Price, L., Riahi, K., Roehrl, A., Rogner, H.-H., Sankovski, A., Schlesinger, M., Shukla, P., Smith, S., Swart, R., van Rooijen, S., Victor, N., and Dadi, Z.: Special Report on Emission Scenarios, Cambridge University Press, 2000.

Oberhuber, J.: Simulation of the Atlantic circulation with a coupled sea ice-mixed layer-isopycnal general circulation model. Part 1:Model description, J. Phys. Oceanogr., 23, 808–829, 1993.

Olivier, J., Bouwman, A., van der Maas, C., Berdowski, J., Veldt, C., Bloos, J., Visschedijk, A., Zandveld, P., and Haverlag, J.: Description of EDGAR Version 2.0: A set of global emission inventories of greenhouse gases and ozone-depleting substances for all anthropogenic and most natural sources on a per country basis and on 1 degree x 1 degree grid, RIVM report, TNO MEP report R96/119, RIVM, Bilthoven, 1996.

Roeckner, E., Arpe, K., Bengtsson, L., Christoph, M., Clausen, M., Dmenil, L., Giorgetta, M., Schlese, U., and Schulzweida, U.: The atmospheric general circulation model ECHAM-4: Model description and simulation of present-day climate., Tech. Rep. 218, Max-Planck-Institut für Meteorologie, 1996.

Roeckner, E., Bengtsson, L., and Feichter, J.: Transient climate change simulations with a coupled atmosphere-ocean GCM including the tropospheric sulfur cycle, J. Climate, 12, 3004–3032, 1999.

Roelofs, G. and Lelieveld, J.: Distribution and budget of O_3 in the troposphere calculated with a chemistry general circulation model, J. Geophys. Res., 100, 20 983–20 998, 1995.

Simpson, D., Fagerli, H., Jonson, J., Tsyro, S., and Wind, P.: Transboundary Acidification, Eutrophication and Ground Level Ozone in Europe, Part 1, Tech. rep., Norwegian Meteorological Institute, available at: www.emep.int, 2003.

Solomon, S., Qin, D., Manning, M., Chen, Z., Marquis, M., Averyt, K., Tignor, M., and Miller, H.: Climate Change 2007: The Physical Science Basis. Contribution of Working Group I to the

Fourth Assessment Report of the Intergovernmental Panel on Climate Change, Tech. rep., Cambridge University Press, Cambridge, United Kingdom and new York, NY, USA, 2007.

Spiegel, M. R.: Theory and problems of Statistics, 2. Ed., Shaum's Outline Series, McGraw-Hill, 1992.

Stendel, M., Schmidt, T., Roeckner, E., and Cubasch, U.: The climate of the 21'st century: Transient simulations with a coupled atmosphere-ocean circulation model, Tech. Rep. 02-1, Danish Climate Centre, Danish Meteorological Institute, 2002.

Taylor, J. R.: An introduction to Error Analysis. The study of uncertainties in physical measurements, 2nd Ed., University Science Books, Sausalito, California, 1997.

Tuovinen, J., Simpson, D., Mayerhofer, P., Lindfors, V., and Laurila, T.: Surface ozone exposures in Northern Europe in changing environmental conditions, in: A Changing Atmosphere: Proceeding of the 8th European Symposium on the Physicco-Chemical Behaviour of the Atmospheric Pollutants, edited by: Hjort, J., Raes, F., and Angeletti, G., DG Research, Joint Research Centre, Paper AP61, European Commission, 2002.

van Loon, M., Roemer, M., Builtjes, P., Bessagnet, B., Rouill, L., Christensen, J., Brandt, J., Fagerli, H., Tarrason, L., Rodgers, I., Stern, R., Bergström, R., Langner, J., and Foltescu, V.: Model inter-comparison. In the framework of the review of the Unified EMEP model, TNO-report, TNO-MEPO-R 282, 2004.

van Loon, M., Vautard, R., Schaap, M., Bergstrm, R., Bessagnet, B., Brandt, J., Builtjes, P., Christensen, J., Cuvelier, K., Graff, A., Jonson, J., Krol, M., Langner, J., Roberts, P., Rouil, L., Stern, R., Tarrasón, L., Thunis, P., Vignati, E., White, L., and Wind, P.: Evaluation of long-term ozone simulations from seven regional air quality models and their ensemble average, Atmos. Environ., 41, 2083–2097, 2007.

Vestreng, V.: Emission data reported to UNECE/EMEP: Evaluation of the spatial distribution of emission, EMEP/MSC-W Note 1/01, EMEP, 2001.

Williamson, D. and Rasch, P.: Water vapor transport in the NCAR CCM2, Tellus, 46A, 34–51, 1994.

Zlatev, Z. and Brandt, J.: Impact of Climate Changes in Europe on European pollution levels, Proceedings from the First ACCENT Symposium, Urbino, Italy, p. 6, 2005.